Title Page.

Expression and functional characterization of breast cancer-associated cytochrome P450 4Z1 in

Saccharomyces cerevisiae

Matthew G. McDonald, Sutapa Ray, Clara J. Amorosi, Katherine A. Sitko, John P. Kowalski, Lorela Paco, Abhinav Nath, Byron Gallis, Rheem A. Totah, Maitreya J. Dunham, Douglas M. Fowler and Allan E. Rettie*

Departments of Medicinal Chemistry (MGM, SR JPK, LP, AN, BG, RAT and AER), Genome Sciences (KAS, CJA, MJD and DMF) and Bioengineering (DMF), University of Washington, Seattle, WA 98195.

Running Title   Catalytic Activity of CYP4Z1

*Address Correspondence to:

Allan E. Rettie, Ph.D.

Department of Medicinal Chemistry

University of Washington, Box 357610

1959 NE Pacific, Seattle WA 98195

Telephone: (206) 685-0615

Fax: (206) 685-3252

Email: rettie@uw.edu

Text pages:	19
Tables:	2
Figures:	6
References:	49
Abstract:	187 words
Introduction:	463 words
Discussion:	943 words

Abbreviations Used

CYP, cytochrome P450; HLM, human liver microsomes; HPLC, high performance liquid

chromatography; LC-MS/MS, liquid chromatography-tandem mass spectrometry; MRM, multiple

reaction monitoring; APCI⁻, atmospheric pressure negative chemical ionization; ESI⁻, negative

electrospray ionization; LA, lauric acid; AA, arachidonic acid; HETE, hydroxyeicosatetraenoic acid;

DHET, dihydroxyeicosatrienoic acid; EET, epoxyeicosatrienoic acid; 15-OH-PDA, 15-

hydroxypentadecanoic acid;

ABSTRACT

CYP4Z1 is an 'orphan' P450 enzyme that has provoked interest because of its hypothesized role in breast cancer through formation of the signaling molecule 20-HETE. We expressed human CYP4Z1 in *Saccharomyces cerevisiae* and evaluated its catalytic capabilities towards arachidonic and lauric acids (AA and LA). Specific and sensitive mass spectrometry assays enabled discrimination of the regioselectivity of hydroxylation of these two fatty acids. CYP4Z1 generated 7-, 8-, 9-, 10- and 11-hydroxy LA, while the 12-hydroxy metabolite was not detected.   HET0016, the prototypic CYP4 inhibitor, only weakly inhibited laurate metabolite formation (IC_{50} ~15 μM). CYP4Z1 preferentially oxidized AA to the 14(S),15(R)-epoxide with high regio- and stereoselectivity, a reaction that was also insensitive to HET0016, but neither 20-HETE nor 20-carboxy-AA were detectable metabolites. Docking of LA and AA into a CYP4Z1 homology model was consistent with this preference for internal fatty acid oxidation. Thus, human CYP4Z1 has an inhibitor profile and product regioselectivity distinct from most other CYP4 enzymes, consistent with CYP4Z1's lack of a covalently-linked heme. These data suggest that, if CYP4Z1 modulates breast cancer progression, it does so by a mechanism other than direct production of 20-HETE.

INTRODUCTION

The CYP4 family in humans contains 12 genes and 13 transcribed enzyme products that typically oxidize fatty acids at their ω-termini (Hsu et al., 2007; Edson and Rettie, 2013). This substrate and product selectivity has been documented extensively for the CYP4A and CYP4F sub-families (Johnston et al., 2011). Indeed, the metabolic conversion of arachidonic acid (AA) to the active signaling molecule, 20-HETE, has physiological relevance in a plethora of tissue types (Fan et al., 2015; Johnson et al., 2015). The importance of this metabolite has been elegantly demonstrated in transgenic mice, where increased formation of 20-HETE caused elevation in blood pressure that could be linked to the functional activities of CYP4A11 and CYP4F2 (Lai et al., 2012; Savas et al., 2016).

In contrast, much less is known about the substrate selectivity of other human CYP4 sub-family members, resulting in many of them being referred to as 'orphan' P450s (Stark and Guengerich, 2007; Kelly et al., 2011). Within the last 10 years, an important physiological role has been established for CYP4F22 (Ohno et al., 2015) and significant progress has been made in better defining the catalytic activities of CYP4F11 (Tang et al., 2010; Edson et al., 2013), CYP4V2 (Nakano et al., 2009; Nakano et al., 2012) and CYP4X1 (Stark et al., 2008).

However, CYP4Z1 is the least well characterized of the CYP4 enzymes. Originally, CYP4Z1 was identified in breast tissue and noted to be up-regulated in breast carcinoma (Rieger et al., 2004). In a more recent study, MCF-7 breast cancer cells exhibited aberrant CYP4Z1 protein targeted to the cell surface, and anti-CYP4Z1 autoantibodies were observed in breast cancer patient, but not control, sera (Nunna et al.). CYP4Z1 expression has also been proposed as a biomarker for the existence of malignancy and/or progression of ovarian and prostate cancer (Downie et al., 2005; Tradonsky et al., 2012). Notably, stable over-expression of CYP4Z1 in breast cancer cells has been reported to promote angiogenesis and tumor growth in mice with a concomitant increase in cellular 20-HETE (Yu et al., 2012). The foregoing studies prompt the hypothesis that CYP4Z1 may act as a prognostic biomarker through generation of 20-HETE in

cancer cells. However, many oxidized metabolites of AA can act as signaling molecules and a full

evaluation of the metabolite profile generated from AA by CYP4Z1 has not been previously performed.

Here, we report the first analysis of AA metabolism by recombinant CYP4Z1 expressed in

Saccharomyces cerevisiae. CYP4Z1 forms no detectable oxidized metabolites at the ω-terminus, but

instead epoxidizes AA at the 14,15-double bond with high regio- and stereo-selectivity. In addition,

CYP4Z1 is relatively insensitive to inhibition by the prototypic CYP4 inhibitor, HET0016. If CYP4Z1

has a role to play in modulating cancer progression, these new data suggest that the mechanism does not

involve direct 20-HETE generation by this enzyme.

MATERIALS and METHODS

General Reagents

18-HETE, 19-HETE, 20-HETE, 20-HETE-d_6, 14,15-EET and 14,15-EET-d_{11} chemical standards were purchased from Cayman Chemical (Ann Arbor, MI). The 9-, 10-, 11- and 12-hydroxy LA standards were previously synthesized (Guan et al., 1998). Recombinant CYP2C19 and CYP4F2 Supersomes, co-expressed in insect cells with cytochrome P450 oxido-reductase (CPR) and cytochrome b5, were procured from Corning Inc. (Corning, N.Y.). The CPR and cytochrome b5 utilized in CYP4Z1 incubations were expressed and purified according to established protocols (Chen et al., 1998). Organic solvents were obtained from Fisher Scientific (Pittsburgh, PA), and all other chemicals (including LA, AA, NADPH, BSTFA, 15-OH PDA, etc.) were purchased from Sigma Aldrich (St. Louis, MO).

Cloning and vector construction

The p41KGAL1 vector was derived from the p416GAL1 vector (Mumberg et al., 1995) and the pUG6 vector (Guldener et al., 1996) using PCR and Gibson assembly to clone the KanMX cassette into p416GAL1 (Supplemental Table 1: primers KAS381, KAS382; KAS378, KAS379). To construct the p41KGAL1_CYP4Z1-HA vector, the *S. cerevisiae* codon-optimized CYP4Z1 sequence (Uniprot: Q86W10) with a C-terminal HA tag (Integrated DNA Technologies) was directionally cloned into the p41KGAL1 vector using SpeI-HF and SalI-HF (New England Biosciences). Ligated plasmids were transformed into F' competent *E. coli* and verified by Sanger sequencing (Supplemental Figure 1: plasmid sequences).

Expression of CYP4Z1 in yeast

The yeast strain YMD3289 (S288C MATα HAP1+ ura3Δ0 leu2Δ1 his3Δ1 trp1Δ63) was transformed with p41KGAL1_CYP4Z1-HA. When required, yeast media was supplemented with 200 µg/mL G418 to maintain the plasmid. Unless otherwise specified, all cultures were grown at 28°C. To

6

induce CYP expression, a single yeast colony was inoculated into 30 mL SC+-Ade medium (synthetic

complete, 2% glucose, 30 mg/L additional adenine) with G418 and grown at 30°C overnight. A 1/100

dilution of the overnight culture was inoculated into 500 mL YPGE medium (10 g/L yeast extract, 20 g/L

peptone, 5 g/L glucose, 3% ethanol) with G418 and grown for 24 hrs at which point 2% galactose (w/v)

was added to induce CYP expression. Cells were grown for an additional 15 h pelleted by centrifugation

for 10 min at 4,000 x g and then frozen at -80°C for microsome preparation.

Western Blotting

One microgram of microsomes from control yeast or from yeast expressing recombinant human

CYP4Z1 were separated on a 4-12% Bis-Tris SDS polyacrylamide gel (Invitrogen) and transferred

electrophoretically to nitrocellulose. After blocking for 2.5 h with 5% w/v BSA, 5% w/v nonfat dry milk

in PBS, 0.1% Triton X-100, the nitroceullose was reacted overnight with a 1:2000 dilution of rabbit anti-

human CYP4Z1 primary antibody (Sigma Atlas) followed by incubation with a 1:10,000 dilution of anti-

rabbit IgG, HRP-linked antibody (Cell Signaling Technology).

Preparation of Yeast Microsomes

Yeast microsomes were prepared as described previously (Pompon et al., 1996) using the

enzymatic breaking procedure and PEG-4000/NaCl method with modifications to buffer volumes.

Harvested cells (~3 g wet weight) were washed with 15 mL TEK buffer (50 mM Tris-HCl pH 7.4, 1 mM

EDTA, 0.1 M KCl), resuspended in 15 mL TEM buffer (50 mM Tris-HCl pH 7.4, 1 mM EDTA, 70 mM

2-mercaptoethanol) and incubated at room temperature for 5-10 min. Cells were recovered and

resuspended in 1.5 mL TMS buffer (1.5 M sorbitol, 20 mM Tris-MES pH 6.3, 2 mM EDTA) and 5 mg

20T Zymolyase was added. Cells were incubated for 1 h at 28°C. Further steps were performed on ice.

Spheroplasts were pelleted at 6,732 x g and washed with 15 mL TES-A buffer (50 mM Tris-HCl pH 7.4,

1 mM EDTA, 1.5 M sorbitol) and the centrifugation step was repeated. Spheroplasts were resuspended in

10 mL TES-B buffer (50 mM Tris-HCl pH 7.4, 1 mM EDTA, 0.6 M sorbitol), and lysed using a Braun

Labsonic U sonicator at a relative output power of 0.25 with 0.9 duty period using 2 x 15 sec pulses. After

waiting 5 min on ice, lysed cells were centrifuged for 4 min at 1,700 x g, and the supernatant was

centrifuged for 10 min at 10,700 x g to remove the mitochondria. The supernatant volume was measured

and TES-B buffer was added to 30 mL total volume. 8 mL 50% PEG 4000 was added dropwise to this

mixture, followed by 2 mL 2.5 M NaCl, and the mixture was incubated on ice for 15 min. The mixture

was then centrifuged for 10 min at 10,700 x g. The microsomal pellet was resuspended in 2 mL TEG

buffer (50 mM Tris-HCl pH 7.4, 1 mM EDTA, 20% (v/v) glycerol) and frozen at -80°C.

CYP4Z1 Quantitation by CO Binding UV-Visible Spectroscopy

Carbon monoxide binding spectra by reduced CYP4Z1 were recorded on an Olis modernized

Aminco DW-2 spectrophotometer (Olis, Bogart, GA). CYP4Z1 yeast microsomes were diluted 2-fold in

50 mM KPi buffer, pH 7.4, containing 20% glycerol, 1 mM EDTA and 0.2% emulgen. Sodium dithionite

(excess, powder) and methyl viologen (1.2 μM) were added and the microsomes were then split equally

between sample and reference quartz cuvettes before taking a baseline scan from 400 to 500 nm, at 25°C.

CO gas was bubbled to saturation through the sample cuvette microsomes, and difference scans were

taken of the CO-bound enzyme. Holo-CYP4Z1 concentrations were calculated according to Beer's law

taking the absorbance difference between the peak maximum (at ~450 nm) and the baseline (at 490 nm),

and using an extinction coefficient of 91 mM^{-1}cm^{-1} (Liu and Franklin, 1985).

General Microsomal Incubation Procedures

AA Assay

CYP4Z1 yeast microsomes (5-15 pmol per reaction), CPR and cytochrome b5 (in a 1:2:1 molar

ratio) were added to 100 mM potassium phosphate buffer, pH 7.4, and incubated on ice for 30 min.

Sodium pyruvate (1 mM final concentration), HET0016 (1 μM, added only for inhibition reactions) and

AA (75 μM) were successively added, and reactions were pre-incubated at 37°C/75 rpm in a water bath

for 3 min prior to initiation through the addition of NADPH (1 mM in a 200 μL final reaction volume). A high AA substrate concentration was chosen to better ensure saturation and facilitate identification of the full complement of metabolites without kinetic concerns. After 15 min incubation, reactions were quenched with 1 mL ethyl acetate, containing 0.01% butylated hydroxytoluene (BHT), and 100 ng each of 20-HETE-d_6 and 14,15-EET-d_{11} were added as internal standards. Reaction mixtures were vortexed, centrifuged and the organic layer collected, and then the extraction process was repeated with another 1 mL of ethyl acetate/BHT. The combined organic layers were evaporated at room temperature under a nitrogen gas stream, and the residue reconstituted in 10 μL of DMSO, with another 40 μL of a 50:50 solution of a 4:1 mix of acetonitrile/methanol in water subsequently added, for LC-MS analysis. Incubations and work-up were all carried out in the dark, and all organic solvents (including those used to make up substrate and standard stock solutions, which were stored at -80ºC) were degassed prior to use. Methanol, from the AA and HET0016 stock solutions, did not exceed 1% of the final reaction volume. Reactions with P450 Supersomes (Corning Inc., Corning, NY) contained 15 pmol P450 enzyme, 1 mM sodium pyruvate, 75 μM AA and 1 mM NADPH in 200 μL of 100 mM potassium phosphate buffer, pH 7.4. Incubation and work-up conditions were identical to those described above for CYP4Z1. Calibration curves were prepared by spiking variable amounts of 18-HETE (for CYP4F12 metabolic analysis) or 19-HETE and 14,15-EET into 200 μL potassium phosphate buffer, containing 1 mM sodium pyruvate, to generate standard mixtures with final concentrations of between 2.5 and 500 pg/μL buffer. These standard solutions, prepared in duplicate, were immediately worked-up and analyzed in an identical fashion to that described for the incubation samples above.

LA Assay

CYP4Z1 yeast microsomes (5-15 pmol per reaction), CPR and cytochrome b5 (in a 1:2:1 molar ratio) were reconstituted in 100 mM potassium phosphate buffer, pH 7.4, and incubated on ice for 30 min, after which LA was added (1 mM final concentration). Reactions were pre-incubated for 3 min at

37ºC/75 rpm in a water bath, prior to initiation through the addition of NADPH (1 mM in a 500 μL final

reaction volume). After 30 min incubation, reactions were quenched with 50 μL of 10% HCl, 10 nmol of

15-OH PDA were added as internal standard, and the solutions were extracted twice with 900 μL of ethyl

acetate. The organic solvent was evaporated under a nitrogen stream, and the residues dissolved in 50 μL

of ethyl acetate. BSTFA reagent (Sigma), 50 μL, was added and the silylation reactions were heated to

90ºC for 60 min. After cooling, the samples were analyzed by GC-MS. Calibration curves were prepared

by spiking concentrated standard mixtures, containing variable amounts of 9, 10, 11 and 12-hydroxy LAs,

into 500 μL of potassium phosphate buffer (0.005 to 25 μM final concentrations). The standard buffer

solutions, prepared in duplicate, were worked-up and analyzed in identical fashion to the incubation

reactions described above.

Analysis of LA Metabolites by GC-MS

GC-MS analyses were performed on a Shimadzu QP2010 Gas Chromatograph Quadrupole Mass

Spectrometer (Shimadzu Scientific, Columbia, MD) using electron impact (EI) ionization. The various

hydroxylated LA metabolites as well as the internal standard, 15-OH PDA, were analyzed as their

respective bis-trimethylsilylated derivatives by selected ion monitoring (SIM) of the following mass

channels: m/z 345 (12-OH LA), m/z 173 (7-OH LA), m/z 159 (8-OH LA), m/z 145 (9-OH LA), m/z 131

(10-OH LA), m/z 117 (11-OH LA) and m/z 387 (15-OH PDA).   The derivatized metabolites were

separated on a Restek Rxi-5Sil MS (fused silica), 30 m, 0.25 μm GC column with 0.25 mm i.d. at an

injection temperature of 250 ºC. The method employed an initial column temperature of 80ºC, which was

held for 0.5 min, and then increased to 160ºC at a rate of 30º/min. From there the rate was slowed to

5º/min up to a temperature of 225ºC and was subsequently increased to 40º/min until reaching a final

temperature of 290ºC. The 9, 10, 11 and 12-hydroxy LA metabolites were quantified by comparing peak

area ratios (relative to the internal standard, 15-OH PDA) to ratios from the appropriate calibration curve,

determined with previously synthesized hydroxy LA standards (Guan et al., 1998), using linear regression

analysis. Since standards of the 7- and 8-hydroxy LAs were unavailable, rates of LA metabolism to these compounds were estimated using the 9-hydroxy LA calibration curve.

Analysis of AA Metabolites by LC-MS/MS

LC-MS/MS analyses were conducted on a Waters Xevo TQ-S Tandem Quadrupole Mass Spectrometer (Waters Co., Milford, MA) coupled to an ACQUITY Ultra Performance LC™ (UPLC™) System with integral autoinjector (Waters). The Xevo was operated in ESI⁻-MS/MS (MRM) mode at a source temperature of 150ºC and a desolvation temperature of 200ºC. The following mass transitions were monitored in separate ion channels for the various oxidative AA metabolites/standards: m/z 337 > 145 (5,6-DHET), m/z 337 > 127 (8,9-DHET), m/z 337 > 167 (11,12-DHET), m/z 337 > 207 (14,15-DHET), m/z 334 > 289 (20-COOH-AA), m/z 330 > 219 (14,15-EET-d_{11}), m/z 325 > 281 (20-HETE-d_6), m/z 319 > 115 (5-HETE), m/z 319 > 155 (8-HETE and 8,9-EET), m/z 319 > 151 (9-HETE), m/z 319 > 167 (11-HETE and 11,12-EET), m/z 319 > 179 (12-HETE and 11,12-EET), m/z 319 > 191 (5,6-EET), m/z 319 > 208 (12-HETE and 11,12-EET), m/z 319 > 219 (15-HETE and 14,15-EET), m/z 319 > 245 (20-HETE), m/z 319 > 247 (17-HETE), m/z 319 > 261 (18-HETE) and m/z 319 > 275 (19-HETE). The cone voltage was set to 20 V for all compounds and optimized collision energies were set to 16 eV for 20-COOH-AA, 17-HETE, 18-HETE, 19-HETE, 20-HETE and 20-HETE-d_6, 10 eV for all other HETEs as well as for all of the EETs, and 15 eV for all DHETs. Note: 17-HETE and 18-HETE metabolite formation was only monitored for CYP4F12 Supersomes (Supplemental Figure 2).

Metabolic products from the AA incubations were separated on an Acquity BEH Shield C_{18}, 1.7 µ, 2.1 x 100 mm, UPLC column (Waters, Corp) using a binary solvent gradient, solvent A: 0.05% aqueous acetic acid and solvent B: 4:1 acetonitrile/methanol plus 0.05% acetic acid, with a constant flow rate of 0.3 mL/min. From 0 to 5.5 min the method was isocratic at 55% B and was then increased to 58% B over 0.5 min. The concentration was maintained at 58% B for another 12 min. Metabolites were quantified through comparison of their peak area ratios (relative to the 20-HETE-d_6 or 14,15-EET-d_{11}

internal standard peak areas) to calibration curves using linear regression analysis. Limits of detection for 19-HETE, 20-HETE and 14,15-EET were below 50 fmol injected on column.

Inhibition of Fatty Acid Metabolism by HET0016

CYP4Z1 (5 pmol), CPR and cytochrome b5 were incubated in potassium phosphate buffer on ice for 30 min, as described. LA (100 μM final concentration) and HET0016 (variable concentration, 0 – 500 μM) were then added from 200 x concentrated methanolic stock solutions. Reactions were incubated and worked-up as previously described for the LA assay. Duplicate incubations were carried out at each inhibitor concentration.

Alternatively, CYP4F12 Supersomes (15 pmol) were incubated with AA (75 μM), sodium pyruvate (1 mM) and NADPH (1 mM) in 200 μL of potassium phosphate buffer for 15 min, as described above for the AA assay, with the addition of HET0016 in the incubation mixtures (at variable concentration, 0 – 500 μM). Again, reactions were incubated and worked-up as previously described and duplicate incubations were carried out at each inhibitor concentration (Supplemental Figure 3).

Preparation of 14,15-EET-Pentafluorobenzyl Ester (PFB) Derivatives

AA metabolites were converted to their pentafluorobenzyl ester derivatives according to the procedure of Mesaros, *et al.* (Mesaros et al., 2010). AA, at 5 μM, was incubated with either CYP4Z1 yeast microsomes or CYP2C19 Supersomes as described above. 14,15-EET-d_{11} (50 ng) was added as internal standard and the incubations were extracted with ethyl acetate/BHT and evaporated under nitrogen. The evaporated residue was reconstituted in 100 μL of dichloromethane (DCM) and 100 μL of a 1:19 solution of diisopropylethyl amine in DCM followed by 100 μL of a 1:9 mixture of pentafluorobenzyl bromide in DCM were subsequently added. The reactions were allowed to shake, in the dark, at room temperature for 30 min, then solvent was removed under a nitrogen stream. Residues were re-solubilized in 300 μL of a 97:3 hexane/ethanol solution for LC-MS/MS analysis.

12

Chiral Resolution and Electron Capture APCI-MS of 14,15-EET-PFB Esters

LC-MS/MS analyses of the derivatized EET-PFB esters were conducted on the Waters Xevo TQ-S MS/ACQUITY UPLC™ System (Waters) described above. The Xevo was operated in APCI⁻-MS/MS (MRM) mode at a source temperature of 150ºC and a probe temperature of 500ºC. The following mass transitions were monitored: m/z 330 > 219 (14,15-EET-d_{11}), m/z 319 > 219 (14,15-EET) with a cone voltage of 40 V and a collision energy of 10 eV set for both channels (under APCI conditions, EET-PFB esters undergo in-source loss of PFB to (re)generate the 14,15-EET anion). The 14,15-EET-PFB enantiomers were resolved on a Chiralpak AD 2.1 x 250 mm, 10 μ column (Daicel Chemical Industries, Ltd., West Chester, PA) at a flow rate of 0.7 mL/min using an isocratic solvent gradient of 98.5% hexane (solvent A) and 1.5% hexane/IPA (4:6, solvent B) as described (Mesaros et al., 2010).

Homology modeling of CYP4Z1 and ligand docking.

A homology model for CYP4Z1 was constructed using the I-TASSER server (Yang et al., 2015), with no templates or experimental constraints specified. The primary template identified by I-TASSER was the CYP4B1 structure (PDB ID: 5T6Q), along with other CYP crystal structures (PDB IDs: 1TQN, 3MDM and 4J14).

Ligand docking was performed in AutoDock Vina (Trott and Olson, 2010). The hydrogen bond weight was doubled to better model the interactions between the carboxylate of the ligands and basic/hydrogen bonding amino acids in the active site, following a previously described protocol for CYP ligand docking (Hsu et al., 2017a). Models of AA and LA were generated in Open Babel (O'Boyle et al., 2011) at pH 7.4 with Gasteiger charges added, and ligand and protein files were processed using AutoDock Tools. The side chains of active site residues of Leu117, Val126, Val379, Asn381, and Ser383 were set to be flexible, while backbone atoms and all other remaining residues (and heme) of the homology model were held rigid. Visualization of the docked ligands in the active site was performed in Chimera (Pettersen et al., 2004).

13

Homology model coordinates have been deposited in the Protein Model Database

(https://bioinformatics.cineca.it/PMDB/) with ID PM0081238.

Data Analysis

Quantitative incubation experiments for measurement of LA and AA CYP4Z1 metabolites were

performed with three replicate samples on two different preparations of yeast microsomes. Due to

enzyme constraints imposed by low CYP4Z1 expression levels, the HET0016 IC_{50} values for inhibition of

LA metabolism were determined in a single experiment using duplicate data points. All other

experiments, unless otherwise indicated, were performed with three replicate samples. Data presented are

means $\pm$ S.D. unless otherwise stated. IC_{50} values were determined in GraphPad Prism v. 7.00 using the

one site fit log(inhibitor) vs response (3 parameters) model.

RESULTS

Characterization of CYP4Z1 expressed in yeast

CYP4Z1 expression in microsomes prepared from *Saccharomyces cerevisiae* was evaluated by SDS-PAGE followed by Western blot analysis using a CYP4Z1 polyclonal peptide antibody. The blot identified a single band at approximately 58 kDa (Figure 1A) in yeast microsomes, which displayed a typical P450 difference spectrum (Figure 1B) following reduction with dithionite and saturation with carbon monoxide. The specific content of CYP4Z1 ranged from 10-20 pmol/mg protein across multiple expression attempts. The exact position of the Soret band could not be determined because of the relatively high ratio of cytochrome c oxidase to CYP4Z1 in these microsomal preparations, which dominated the Soret region of CO binding spectra of microsomes prepared from empty vector controls (not shown).

Metabolism of lauric acid by CYP4Z1

First, we evaluated CYP4Z1-dependent metabolism of LA because medium-chain saturated fatty acids are the only substrates for the enzyme to have been examined, albeit in whole yeast cells (Zollner et al., 2009). CYP4Z1-expressing yeast microsomes incubated with LA and NADPH generated five internal alcohol metabolites, but none of the terminal 12-hydroxy metabolite (Figure 2). Alcohols were analyzed by gas chromatography-mass spectrometry as their trimethylsilyl derivatives, which permitted unambiguous assignment of the biologically-generated 7-OH, 8-OH, 9-OH, 10-OH and 11-OH metabolites from their characteristic fragmentations. Formation of mid-chain LA alcohols by CYP4Z1 was expected because the 7-OH, 8-OH, 9-OH and 10-OH metabolites are also generated by CYP4Z1-expressing *Schizosaccharomyces pombe* cells (Zollner et al., 2009). However, our findings expand the CYP4Z1 metabolite profile to include 11-OH LA, generated by CYP4Z1-expressing yeast microsomes. The 7-OH, 8-OH, 9-OH, 10-OH and 11-OH LAs were formed in a ratio of ~1:20:3:8:4 (Table 1). Although, HET0016 is a nanomolar inhibitor of most CYP4 enzymes, it inhibited CYP4Z1-mediated LA 8-, 9- and10-hydroxylation relatively weakly with an average IC_{50} of 15 μM (Figure 3).

15

Metabolism of arachidonic acid by CYP4Z1

P450 enzymes can transform AA into a plethora of metabolites, as exemplified by the diversity of regioisomeric EETs and HETEs generated by CYP2C19 (Figure 4, upper panel). In contrast, NADPH-supplemented CYP4Z1 microsomes formed only (cis) 14,15-EET and a trace amount of 19-HETE (Figure 4, lower panel; Table 1). CYP4Z1 formed no detectable 20-HETE or 20-carboxy AA metabolites, despite the fact that these are prominent metabolites of CYP4F2 (Figure 4, middle panel). Similar to metabolism of LA, HET0016 was not an effective inhibitor of CYP4Z1-catalyzed AA metabolism, showing no inhibition at the commonly used concentration of 1 μM (Figure 4, lower panel). Finally, we evaluated the stereochemistry of the major 14,15-EET metabolite generated by CYP4Z1. Chiral-phase analysis demonstrated that CYP4Z1 generated the *cis*-14(S),15(R)-EET with 80% enantiomeric excess (Figure 5). Stereochemistry was assigned on the basis of the relative elution of 14,15-EET enantiomers produced by CYP2C19, as reported previously (Mesaros et al., 2010).

Homology modeling of CYP4Z1 and ligand docking.

The homology model for CYP4Z1 shows an active site containing the hydrophobic amino acid residues Leu117, Val126 and Val379 that help confine aliphatic regions of fatty acid substrates. Towards the 'mouth' of this substrate-binding pocket are the hydrogen bonding residues Asn381 and Ser383 (Figure 6A, B). The highest affinity lauric acid pose is situated with the -1,2,3,4 positions all within close proximity to the heme iron, with measured distances of 5.0, 4.7, 3.7, and 4.7 Å. These correspond to the 11-,10-,9-, and 8-OH products, respectively. The highest affinity pose generated for arachidonic acid is positioned for 14,15-EET production, with carbons 14 and 15 situated 4.9 Å and 6.1 Å, respectively, from the heme iron (Figure 6B). The carboxylate moieties of arachidonic and lauric acids are located 2.4 Å and 1.9 Å, respectively, from Asn381, suggesting that hydrogen-bonding interactions with this amino acid may serve to position the internal aliphatic sections of the substrates over the heme for oxidation. Although Ser383 is located, respectively, 4.7 Å and 6.4 Å away from the LA and AA carboxylate

moieties in these models, other slightly lower affinity configurations place the residue within hydrogen-

bonding distance of the acid groups (not shown), suggesting that Ser383 might also play a role in

positioning the fatty acids within the CYP4Z1 active site. Given the limitations of homology modeling

and computational docking, these poses should not be regarded as atomically precise. Instead, they

represent plausible models of CYP4Z1/substrate complexes that are fully consistent with our

experimental data.

DISCUSSION

Prior to our work the only data available regarding catalysis by CYP4Z1 was obtained from expression of the enzyme in *Schizosaccharomyces pombe* followed by whole-cell biotransformation studies with lauric and myristic acids (Zollner et al., 2009), and in microsomes from T47D cells that had been transfected with CYP4Z1 (Yu et al., 2012). The former efforts identified *internal* monohydroxylated fatty acid metabolites rather than formation of the expected ω-hydroxy products by CYP4Z1. The microsomal studies reported here, with budding yeast-expressed CYP4Z1, confirm the formation of several mid-chain alcohols from LA and extend the metabolite profile to include 11-OH LA. This somewhat unusual profile for a CYP4 enzyme is, nonetheless, in-line with expectations based on the absence of a heme covalent link in CYP4Z1 (Table 2). The covalent link cannot exist in this enzyme because CYP4Z1 lacks the I-helix glutamic acid residue that forges an ester bond with the heme (LeBrun et al., 2002; Zheng et al., 2003). Instead, CYP4Z1 has an alanine at this position (Table 2). The reported substrate selectivity of CYP4F8, CYP4F12 and CYP4X1 supports this theory as each of these enzymes also lack the I-helix glutamate residue and have likewise been shown to prefer internal rather than ω-fatty acid oxidation of arachidonic acid (Table 2),

Given the structural argument above, 20-HETE generation by CYP4Z1 as reported by Yu et al., (2012), seemed unusual and so we examined the full metabolite profile of AA by LC-MS/MS. These studies revealed 14,15-EET to be the major metabolite, with no evidence for 20-HETE production. Cognizant of the differences between the two studies, we went to extreme lengths to ensure that we were not overlooking, or mis-assigning, a 20-HETE pathway in CYP4Z1-expressing yeast microsomes. First, we developed a recombinant expression system that provided demonstrably active CYP4Z1 (via the generated CO-difference spectrum) in the microsomal preparations used for the metabolic studies. Second, we confirmed that our microsomal enzyme preparations recapitulated the internal hydroxylations of lauric acid that were expected based on, (i) an earlier study in whole yeast cells (Zollner et al., 2009), and (ii) the structural features of the enzyme. Third, we developed a highly sensitive and highly specific

LC-MS/MS assay for 20-HETE that had a limit of detection of 50 fmol on column, equivalent to a turnover rate of ~5 pmol/min/nmol CYP4Z1. Therefore, if CYP4Z1 generated 20-HETE in any significant amount, we would have observed it. Additionally, since we found earlier that CYP4F2 could sequentially metabolize vitamin K to a terminal acid metabolite (Edson et al., 2013), we considered the possibility that CYP4Z1 might convert 20-HETE to 20-carboxy-AA. However, LC-MS/MS analysis did not support this scenario, despite an appropriate enzyme control (CYP4F2). A final control was re-investigation of the AA metabolite profile generated by CYP4F12, which also lacks a heme covalent link. As expected, we found that this enzyme generated 18-HETE instead of 20-HETE as the major hydroxylated metabolite (Supplemental Figure 2), further validating our analytical procedures. In the aggregate, our studies provide convincing evidence *against* ω-hydroxylation of fatty acids by CYP4Z1, in-line with the evolving structure-function relationships for CYP4 enzymes that cannot forge a covalent heme link. Reasons for the differences between the two studies are unknown at this time, but may reflect the varied cell systems and /or analytical procedures employed. Additional studies with purified reconstituted CYP4Z1 are needed to fully define the enzyme's substrate and product specificities.

Interestingly, CYP4Z1 also demonstrates relatively modest inhibition by the prototypic CYP4 inhibitor, HET0016. CYP4 enzymes that are committed ω-hydroxylases typically exhibit IC_{50} values for this formamidoxime inhibitor that are less than 100 nM (Parkinson et al., 2012; Edson and Rettie, 2013). However, HET0016 inhibited LA hydroxylation catalyzed by CYP4Z1 with an IC_{50} of only 15 μM. Presumably, the structural features that promote ω-hydroxylation by most CYP4 enzymes (Hsu et al., 2017b) also impart tighter binding and inhibition by HET0016. We attempted to test this hypothesis by looking at HET0016 inhibition of AA metabolism by CYP4F12 Supersomes – the only commercially available CYP4 enzyme lacking the I-helix glutamate residue that enables formation of the covalent heme link. We were able to confirm literature reports that CYP4F12 primarily metabolizes AA to 18-HETE with little to no 20-HETE formation (Stark et al., 2005), although we did also observe the production of 17-HETE and 19-HETE as minor metabolites (Supplemental Figure 2). HET0016 inhibited CYP4F12-

mediated AA metabolism with an IC_{50} of ~600 nM (Supplemental Figure 3). While this value is significantly lower than what we observed for HET0016 inhibition of CYP4Z1-mediated LA metabolism, it is still ~10-fold higher than literature values reported for HET0016 inhibition of more typical CYP4 ω-hydroxylase enzymes. More extensive studies with other CYP4 enzymes lacking the heme covalent link are needed to confirm this apparent co-segregation.

While both 20-HETE production and CYP4 enzyme expression are increased in a number of human cancers (Alexanian et al., 2012), our findings are suggestive of a role for 14,15-EET in these malignant events, in accord with several literature reports (Jiang et al., 2007; Mitra et al., 2011; Wei et al., 2014). Indeed, a specific role for racemic 14,15-EET, formed by CYP3A4 and acting to mediate breast cancer cell growth through Stat3, has been advanced (Mitra et al., 2011). In preliminary studies, we have confirmed that CYP3A4 forms 14,15-EET with little stereochemical bias (data not shown). Therefore, since CYP4Z1 formed 14(S),15(R)-EET with high stereoselectivity, it will be interesting to contrast the effects of the two epoxide enantiomers on breast cancer cell growth and invasiveness. Finally, our data provide a cautionary note about the use of HET0016 as a pan-CYP4 inhibitor, particularly at low micromolar concentrations in cellular studies to diagnose involvement of CYP4 enzymes that do not possess a covalently modified heme.

Authorship Contributions

Participated in research design: Fowler, Dunham, McDonald, Rettie

Conducted experiments: McDonald, Amorosi, Ray, Sitko

Contributed new reagents or analysis tools: Totah, Gallis, Kowalski, Paço, Nath

Performed data analysis: McDonald, Ray, Rettie

Wrote or contributed to the writing of the manuscript: McDonald, Fowler, Rettie

REFERENCES

Alexanian A, Miller B, Roman RJ and Sorokin A (2012) 20-HETE-producing enzymes are up-regulated in human cancers. *Cancer Genomics Proteomics* **9:**163-169.

Bylund J, Bylund M and Oliw EH (2001) cDna cloning and expression of CYP4F12, a novel human cytochrome P450. *Biochem Biophys Res Commun* **280:**892-897.

Bylund J, Hidestrand M, Ingelman-Sundberg M and Oliw EH (2000) Identification of CYP4F8 in human seminal vesicles as a prominent 19-hydroxylase of prostaglandin endoperoxides. *J Biol Chem* **275:**21844-21849.

Chen W, Koenigs LL, Thompson SJ, Peter RM, Rettie AE, Trager WF and Nelson SD (1998) Oxidation of acetaminophen to its toxic quinone imine and nontoxic catechol metabolites by baculovirus-expressed and purified human cytochromes P450 2E1 and 2A6. *Chem Res Toxicol* **11:**295-301.

Christmas P, Jones JP, Patten CJ, Rock DA, Zheng Y, Cheng SM, Weber BM, Carlesso N, Scadden DT, Rettie AE and Soberman RJ (2001) Alternative splicing determines the function of CYP4F3 by switching substrate specificity. *J Biol Chem* **276:**38166-38172.

Downie D, McFadyen MC, Rooney PH, Cruickshank ME, Parkin DE, Miller ID, Telfer C, Melvin WT and Murray GI (2005) Profiling cytochrome P450 expression in ovarian cancer: identification of prognostic markers. *Clin Cancer Res* **11:**7369-7375.

Edson KZ, Prasad B, Unadkat JD, Suhara Y, Okano T, Guengerich FP and Rettie AE (2013) Cytochrome P450-dependent catabolism of vitamin K: omega-hydroxylation catalyzed by human CYP4F2 and CYP4F11. *Biochemistry* **52:**8276-8285.

Edson KZ and Rettie AE (2013) CYP4 enzymes as potential drug targets: focus on enzyme multiplicity, inducers and inhibitors, and therapeutic modulation of 20-hydroxyeicosatetraenoic acid (20-HETE) synthase and fatty acid omega-hydroxylase activities. *Curr Top Med Chem* **13:**1429-1440.

Fan F, Muroya Y and Roman RJ (2015) Cytochrome P450 eicosanoids in hypertension and renal disease. *Curr Opin Nephrol Hypertens* **24:**37-46.

Fer M, Corcos L, Dreano Y, Plee-Gautier E, Salaun JP, Berthou F and Amet Y (2008) Cytochromes P450 from family 4 are the main omega hydroxylating enzymes in humans: CYP4F3B is the prominent player in PUFA metabolism. *J Lipid Res* **49:**2379-2389.

Guan X, Fisher MB, Lang DH, Zheng YM, Koop DR and Rettie AE (1998) Cytochrome P450-dependent desaturation of lauric acid: isoform selectivity and mechanism of formation of 11-dodecenoic acid. *Chem Biol Interact* **110:**103-121.

Guldener U, Heck S, Fielder T, Beinhauer J and Hegemann JH (1996) A new efficient gene disruption cassette for repeated use in budding yeast. *Nucleic Acids Res* **24:**2519-2524.

Hsu MH, Baer BR, Rettie AE and Johnson EF (2017a) The Crystal Structure of Cytochrome P450 4B1 (CYP4B1) Monooxygenase Complexed with Octane Discloses Several Structural Adaptations for omega-Hydroxylation. *J Biol Chem* **292:**5610-5621.

Hsu MH, Baer BR, Rettie AE and Johnson EF (2017b) The Crystal Structure of Cytochrome P450 4B1 (CYP4B1) Monoxygenase Complexed with Octane Discloses Several Structural Adaptations for omega-Hydroxylation. *J Biol Chem*.

Hsu MH, Savas U, Griffin KJ and Johnson EF (2007) Human cytochrome p450 family 4
enzymes: function, genetic variation and regulation. *Drug Metab Rev* **39:**515-538.

Jiang JG, Ning YG, Chen C, Ma D, Liu ZJ, Yang S, Zhou J, Xiao X, Zhang XA, Edin ML, Card JW,
Wang J, Zeldin DC and Wang DW (2007) Cytochrome p450 epoxygenase promotes
human cancer metastasis. *Cancer Res* **67:**6665-6674.

Johnson AL, Edson KZ, Totah RA and Rettie AE (2015) Cytochrome P450 omega-
Hydroxylases in Inflammation and Cancer. *Adv Pharmacol* **74:**223-262.

Johnston JB, Ouellet H, Podust LM and Ortiz de Montellano PR (2011) Structural control of
cytochrome P450-catalyzed omega-hydroxylation. *Arch Biochem Biophys* **507:**86-94.

Kelly EJ, Nakano M, Rohatgi P, Yarov-Yarovoy V and Rettie AE (2011) Finding homes for
orphan cytochrome P450s: CYP4V2 and CYP4F22 in disease states. *Mol Interv*
11:124-132.

Lai G, Liu X, Wu J, Liu H and Zhao Y (2012) Evaluation of CMV and KAP promoters for
driving the expression of human CYP4F2 in transgenic mice. *Int J Mol Med* **29:**107-
112.

LeBrun LA, Xu F, Kroetz DL and Ortiz de Montellano PR (2002) Covalent attachment of the
heme prosthetic group in the CYP4F cytochrome P450 family. *Biochemistry*
41:5931-5937.

Liu Z and Franklin MR (1985) Cytochrome P-450 ligands: metyrapone revisited. *Arch
Biochem Biophys* **241:**397-402.

Mesaros C, Lee SH and Blair IA (2010) Analysis of epoxyeicosatrienoic acids by chiral liquid
chromatography/electron capture atmospheric pressure chemical ionization mass

spectrometry using [13C]-analog internal standards. *Rapid Commun Mass Spectrom* **24:**3237-3247.

Mitra R, Guo Z, Milani M, Mesaros C, Rodriguez M, Nguyen J, Luo X, Clarke D, Lamba J, Schuetz E, Donner DB, Puli N, Falck JR, Capdevila J, Gupta K, Blair IA and Potter DA (2011) CYP3A4 mediates growth of estrogen receptor-positive breast cancer cells in part by inducing nuclear translocation of phospho-Stat3 through biosynthesis of (+/-)-14,15-epoxyeicosatrienoic acid (EET). *J Biol Chem* **286:**17543-17559.

Mumberg D, Muller R and Funk M (1995) Yeast vectors for the controlled expression of heterologous proteins in different genetic backgrounds. *Gene* **156:**119-122.

Nakano M (2011) Biochemical characterization of CYP4V2 and its role in the retinal disease, Biettie Crystalline Dystrophy, University of Washington.

Nakano M, Kelly EJ and Rettie AE (2009) Expression and characterization of CYP4V2 as a fatty acid omega-hydroxylase. *Drug Metab Dispos* **37:**2119-2122.

Nakano M, Kelly EJ, Wiek C, Hanenberg H and Rettie AE (2012) CYP4V2 in Bietti's crystalline dystrophy: ocular localization, metabolism of omega-3-polyunsaturated fatty acids, and functional deficit of the p.H331P variant. *Mol Pharmacol* **82:**679-686.

Nunna V, Jalal N and Bureik M Anti-CYP4Z1 autoantibodies detected in breast cancer patients. *Cell Mol Immunol.*

O'Boyle NM, Banck M, James CA, Morley C, Vandermeersch T and Hutchison GR (2011) Open Babel: An open chemical toolbox. *J Cheminform* **3:**33.

Ohno Y, Nakamichi S, Ohkuni A, Kamiyama N, Naoe A, Tsujimura H, Yokose U, Sugiura K, Ishikawa J, Akiyama M and Kihara A (2015) Essential role of the cytochrome P450

CYP4F22 in the production of acylceramide, the key lipid for skin permeability barrier formation. *Proc Natl Acad Sci U S A* **112:**7707-7712.

Parkinson OT, Kelly EJ, Bezabih E, Whittington D and Rettie AE (2012) Bioactivation of 4-Ipomeanol by a CYP4B enzyme in bovine lung and inhibition by HET0016. *J Vet Pharmacol Ther* **35:**402-405.

Pettersen EF, Goddard TD, Huang CC, Couch GS, Greenblatt DM, Meng EC and Ferrin TE (2004) UCSF Chimera--a visualization system for exploratory research and analysis. *J Comput Chem* **25:**1605-1612.

Pompon D, Louerat B, Bronine A and Urban P (1996) Yeast expression of animal and plant P450s in optimized redox environments. *Methods Enzymol* **272:**51-64.

Powell PK, Wolf I, Jin R and Lasker JM (1998) Metabolism of arachidonic acid to 20-hydroxy-5,8,11, 14-eicosatetraenoic acid by P450 enzymes in human liver: involvement of CYP4F2 and CYP4A11. *J Pharmacol Exp Ther* **285:**1327-1336.

Rieger MA, Ebner R, Bell DR, Kiessling A, Rohayem J, Schmitz M, Temme A, Rieber EP and Weigle B (2004) Identification of a novel mammary-restricted cytochrome P450, CYP4Z1, with overexpression in breast carcinoma. *Cancer Res* **64:**2357-2364.

Savas U, Wei S, Hsu MH, Falck JR, Guengerich FP, Capdevila JH and Johnson EF (2016) 20-Hydroxyeicosatetraenoic Acid (HETE)-dependent Hypertension in Human Cytochrome P450 (CYP) 4A11 Transgenic Mice: NORMALIZATION OF BLOOD PRESSURE BY SODIUM RESTRICTION, HYDROCHLOROTHIAZIDE, OR BLOCKADE OF THE TYPE 1 ANGIOTENSIN II RECEPTOR. *J Biol Chem* **291:**16904-16919.

Stark K, Dostalek M and Guengerich FP (2008) Expression and purification of orphan cytochrome P450 4X1 and oxidation of anandamide. *FEBS J* **275:**3706-3717.

Stark K and Guengerich FP (2007) Characterization of orphan human cytochromes P450. *Drug Metab Rev* **39:**627-637.

Stark K, Wongsud B, Burman R and Oliw EH (2005) Oxygenation of polyunsaturated long chain fatty acids by recombinant CYP4F8 and CYP4F12 and catalytic importance of Tyr-125 and Gly-328 of CYP4F8. *Arch Biochem Biophys* **441:**174-181.

Tang Z, Salamanca-Pinzon SG, Wu ZL, Xiao Y and Guengerich FP (2010) Human cytochrome P450 4F11: heterologous expression in bacteria, purification, and characterization of catalytic function. *Arch Biochem Biophys* **494:**86-93.

Tradonsky A, Rubin T, Beck R, Ring B, Seitz R and Mair S (2012) A search for reliable molecular markers of prognosis in prostate cancer: a study of 240 cases. *Am J Clin Pathol* **137:**918-930.

Trott O and Olson AJ (2010) AutoDock Vina: improving the speed and accuracy of docking with a new scoring function, efficient optimization, and multithreading. *J Comput Chem* **31:**455-461.

Wei X, Zhang D, Dou X, Niu N, Huang W, Bai J and Zhang G (2014) Elevated 14,15-epoxyeicosatrienoic acid by increasing of cytochrome P450 2C8, 2C9 and 2J2 and decreasing of soluble epoxide hydrolase associated with aggressiveness of human breast cancer. *BMC Cancer* **14:**841.

Yang J, Yan R, Roy A, Xu D, Poisson J and Zhang Y (2015) The I-TASSER Suite: protein structure and function prediction. *Nat Methods* **12:**7-8.

Yu W, Chai H, Li Y, Zhao H, Xie X, Zheng H, Wang C, Wang X, Yang G, Cai X, Falck JR and Yang J (2012) Increased expression of CYP4Z1 promotes tumor angiogenesis and growth in human breast cancer. *Toxicol Appl Pharmacol* **264:**73-83.

Zheng YM, Baer BR, Kneller MB, Henne KR, Kunze KL and Rettie AE (2003) Covalent heme

binding to CYP4B1 via Glu310 and a carbocation porphyrin intermediate.

Biochemistry **42:**4601-4606.

Zollner A, Dragan CA, Pistorius D, Muller R, Bode HB, Peters FT, Maurer HH and Bureik M

(2009) Human CYP4Z1 catalyzes the in-chain hydroxylation of lauric acid and

myristic acid. *Biol Chem* **390:**313-317.

Footnotes

FIGURE LEGENDS

Figure 1: Characterization of CYP4Z1 expressed in yeast microsomes.   A) Western blot of

microsomes harvested from un-transformed yeast (lane 1) and from yeast expressing CYP4Z1 (lane 2).

B) Carbon monoxide difference spectrum of reduced CYP4Z1 microsomes.

Figure 2: GC-MS chromatogram of LA metabolites generated by recombinant CYP4Z1. The

chromatograms show resolution of the hydroxylated products generated from incubations of LA with

CYP4Z1-expressing yeast microsomes, in the presence (bottom traces) and absence (top traces) of

NADPH cofactor (LA metabolites were quantitatively converted to their (bis)trimethylsilyl derivatives

prior to analysis). Individual metabolites were identified by selected ion monitoring (SIM) of the optimal,

differentiating mass fragmentation ions for each derivatized regioisomer (7-OH LA, m/z = 173; 8-OH LA,

m/z = 159; 9-OH LA, m/z = 145; 10-OH LA, m/z = 131; 11-OH LA, m/z = 117 and 12-OH LA, m/z =

345). 12-OH LA (Rt = 15.6 min) concentrations were below the limit of detection (i.e. < 0.02 pmol were

produced/min/pmol CYP4Z1).

Figure 3: HET0016 inhibition of CYP4Z1-catalyzed LA metabolism. The overlaid graphs show the

relative IC_{50} curves for inhibition of yeast microsomal CYP4Z1-mediated LA 8-, 9- and 10-hydroxylase

activity by HET0016, a low nM inhibitor of most CYP4 enzymes. Data points denote the mean turnover

rate of LA to each metabolite, obtained from duplicate incubations of 100 μM LA and HET0016 (at

concentrations ranging from 0.1 – 500 μM) with CYP4Z1 microsomes, expressed as a percentage of the

rate obtained in the absence of inhibitor. HET0016 inhibited formation of 8-OH LA, 9-OH LA and 10-

OH LA with IC_{50} values of 14.7, 14.9 and 15.9 μM, respectively (we were unable to generate reasonable

IC_{50} curves in this experiment for either 7-OH LA, due to low turnover rates, or 11-OH LA, due to

overlap of the derivatized metabolite peak with HET0016).

Figure 4: ESI⁻ LC-MS/MS chromatograms of AA metabolism by cytochrome P450s. Total ion chromatograms (TICs) of metabolites produced from incubations of 75 μM AA with CYP2C19 and CYP4F2 Supersomes and with CYP4Z1 yeast microsomes, in the presence and absence of NADPH (TICs = sum of 17 individual AA metabolite MRM channels plus channels for the internal standards, 20-HETE-d_6 and 14,15-EET-d_{11}). An additional TIC is included to show (the lack of) HET0016 inhibition of CYP4Z1 AA metabolism at 1 μM HET0016. Insets represent magnifications of individual MRM chromatograms from the (+) NADPH incubations of P450 with AA (peaks are normalized to the same scale): A) $m/z = 325 > 281$ (20-HETE-d_6) B) $m/z = 333 > 271$ (20-COOH-AA) C) $m/z = 319 > 245$ (20-HETE) D) $m/z = 319 > 275$ (19-HETE).

Figure 5: LC-MS/MS chromatograms showing stereoselective formation of 14,15-EET by CYP4Z1 and CYP2C19. The chromatograms show chiral resolution of the 14,15-EET metabolic products isolated from incubations of AA with either CYP4Z1 yeast microsomes or CYP2C19 Supersomes (with (±)14,15-EET-d_{11} added as internal standard). Metabolites and standards were derivatized to their pentafluorobenzyl (PFB) esters and then analyzed by electron capture APCI⁻ LC-MS/MS (resolution was achieved on a Chiralpak AD column).

Figure 6: 3D Homology models of the CYP4Z1 active site with LA and AA docked. The CYP4Z1 amino acid residues shown in light blue are believed to be of primary importance to substrate binding, with Leu117, Val126 and Val379 forming a hydrophobic pocket encapsulating the fatty chains of LA (green, panel A) and AA (lavender, panel B). Asn381 appears to anchor both substrates in the active site, likely through electrostatic interactions formed between the Asn amine and the fatty acid carboxylate moieties (~ 2 Å distant). A) The model of LA bound to CYP4Z1 shows internal carbons of the fatty acid centered over the heme (brown), with C-8 through C-11 of LA all located between 3.7-5.0 Å from the heme iron atom. By contrast, the terminal carbon of LA is oriented away from the heme iron at a distance

of 6.3 Å. B) The model of AA bound to CYP4Z1 likewise shows the terminal carbon of the fatty acid to be pointed away from the heme, while the C_{14}-C_{15} double bond of AA is only 5-6 Å distant from the heme iron. In the figure, oxygen atoms are shown in red, nitrogen atoms are in dark blue, sulfur atoms are in yellow and the heme iron is shown as a brown sphere.

Table 1. Rates of lauric acid (LA) and arachidonic acid (AA) metabolite formation by CYP4Z1 microsomes.

Substrate[a]	Metabolite	Rate (pmol/pmol/min)
LA	7-OH LA	~2[b]
LA	8-OH LA	~40[b]
LA	9-OH LA	6.1 ± 0.7
LA	10-OH LA	16.0 ± 1.4
LA	11-OH LA	8.8 ± 0.2
LA	12-OH LA	n.d.
AA	19-HETE	0.048 ± 0.004
AA	20-HETE	n.d.
AA	20-COOH-AA	n.d.
AA	14,15-EET	1.9 ± 0.06

[a] Substrate concentrations: 1 mM LA; 75 μM AA

[b] Since we lacked synthetic standards for the 7- and 8-hydroxy metabolites of LA, these values were estimated using the 9-OH LA calibration curve.
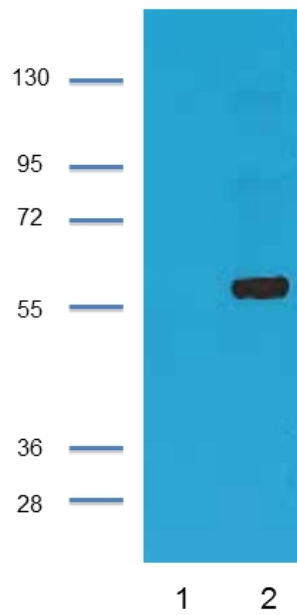
n.d. = not detected

Table 2: Relationship between the presence of a predicted heme covalent link and 20-HETE

formation in human CYP4 enzymes

Sub-family	Enzyme	Localization	Covalent Heme	Arachidonic acid metabolite
CYP4A	4A11	Liver, kidney	Yes (F**E**GHDT)	20-HETE (Powell et al., 1998)
	4A22	Liver, kidney	Yes (F**E**GHDT)	-
CYP4FB	4B1	Lung, bladder	Yes (F**E**GHDT)	-
CYP4V	4V2	Retina	Yes (F**E**GHDT)	20-HETE (Nakano, 2011)
CYP4F	4F2	Liver, kidney	Yes (F**E**GHDT)	20-HETE (Powell et al., 1998)
	4F3A	Myeloid tissues	Yes (F**E**GHDT)	20-HETE (Fer et al., 2008)
	4F3B	Liver, kidney	Yes (F**E**GHDT)	20-HETE (Christmas et al., 2001)
	4F11	Liver, kidney	Yes (F**E**GHDT)	20-HETE (Tang et al., 2010)
	4F22	Skin	Yes (F**E**GHDT)	-
	4F8	Urogenital	**No** (F**G**GHDT)	**18-HETE (Bylund et al., 2000)**
	4F12	Liver, intestine	**No** (F**G**GHDT)	**18-HETE (Bylund et al., 2001)**
CYP4X	**4X1**	Brain, skin	**No** (L**A**GHDT)	**14,15-EET (Stark et al., 2008)**
CYP4Z	**4Z1**	Breast tissue	**No** (F**A**GHDT)	**20-HETE (Yu et al., 2012)**
	4Z1	Breast tissue	**No** (F**A**GHDT)	**14,15-EET (Current study)**

Figure 1

A.

B.
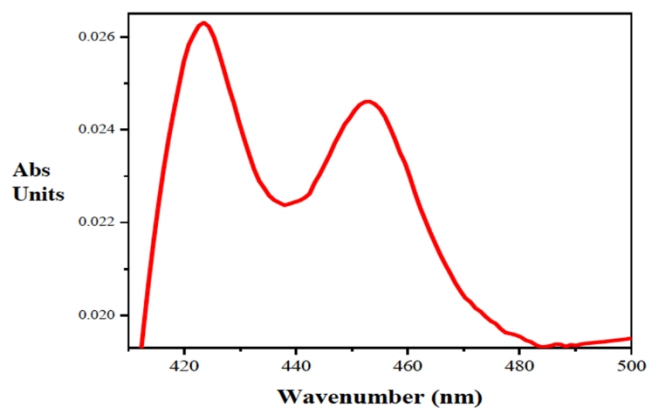
Figure 2.

Figure 3.

Figure 4.

Metabolite Peaks
1. 14,15-DHET
2. 11,12-DHET
3. 8,9-DHET
4. 5,6-DHET
5. 19-HETE
6. 20-HETE-d_6
7. 20-HETE
8. 15-HETE
9. 11-HETE
10. 8-HETE
11. 12-HETE
12. 9-HETE
13. 5-HETE
14. 14,15-EET-d_{11}
15. 14,15-EET
16. 11,12-EET
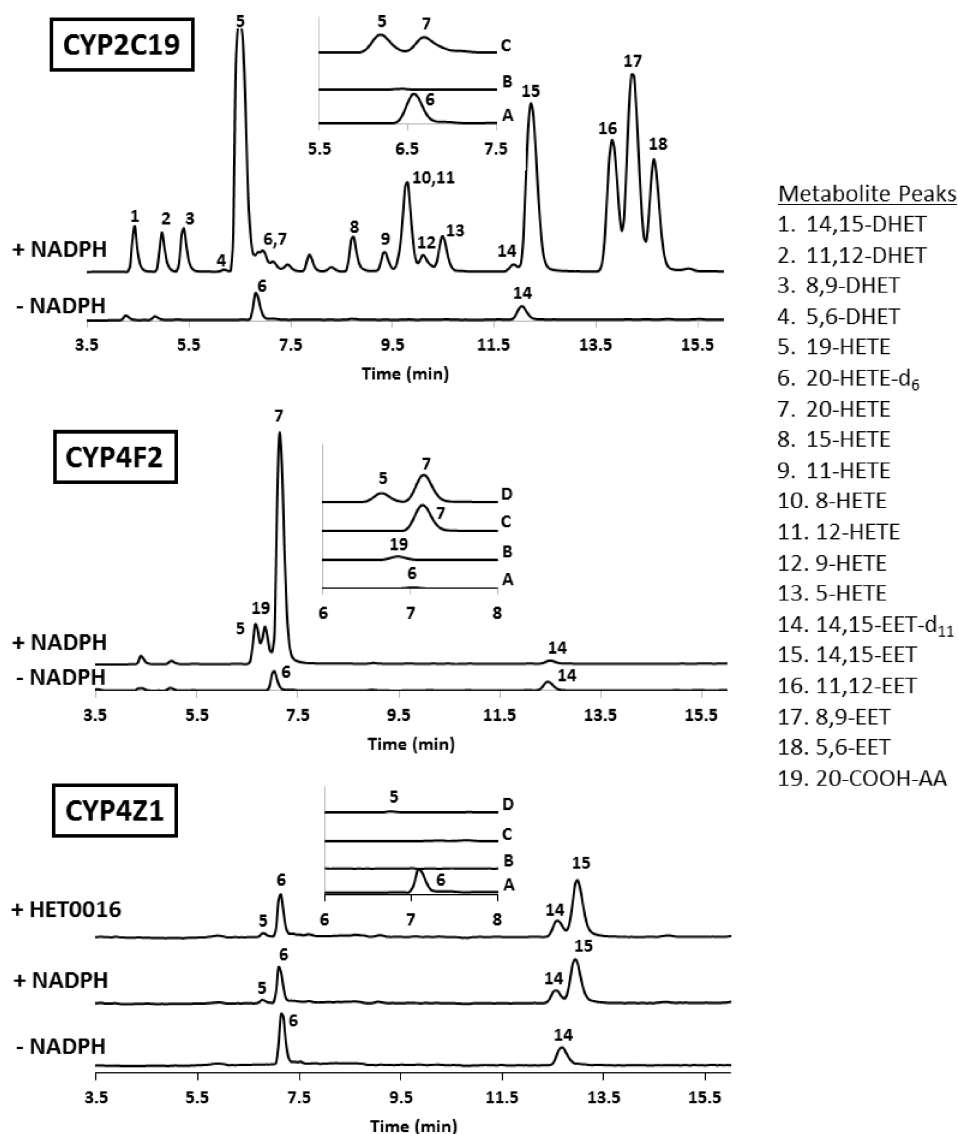17. 8,9-EET
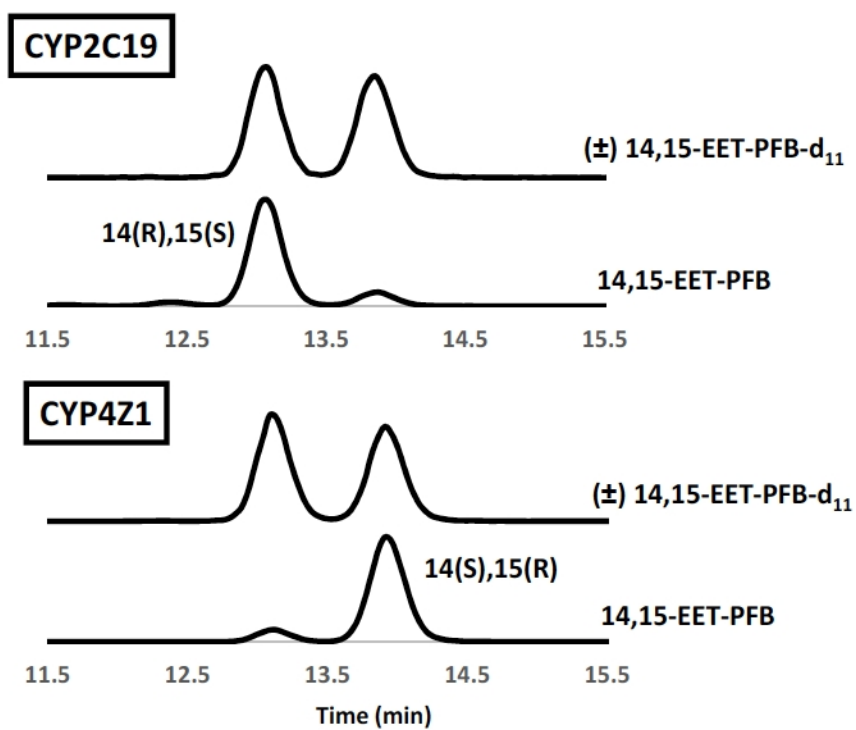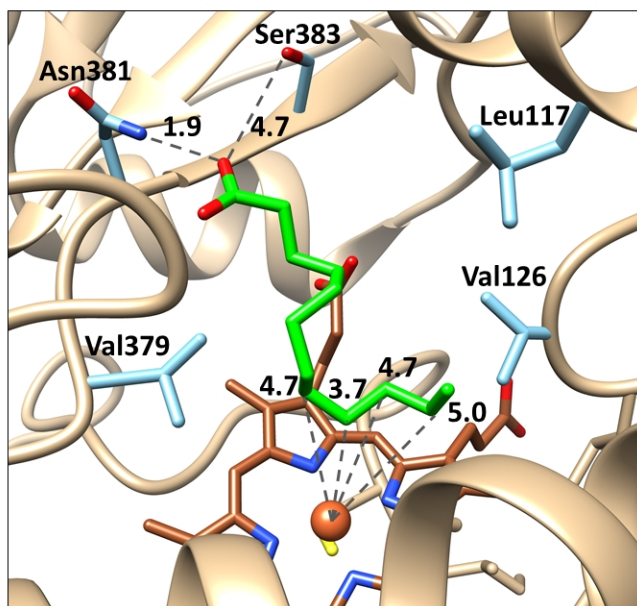18. 5,6-EET
19. 20-COOH-AA
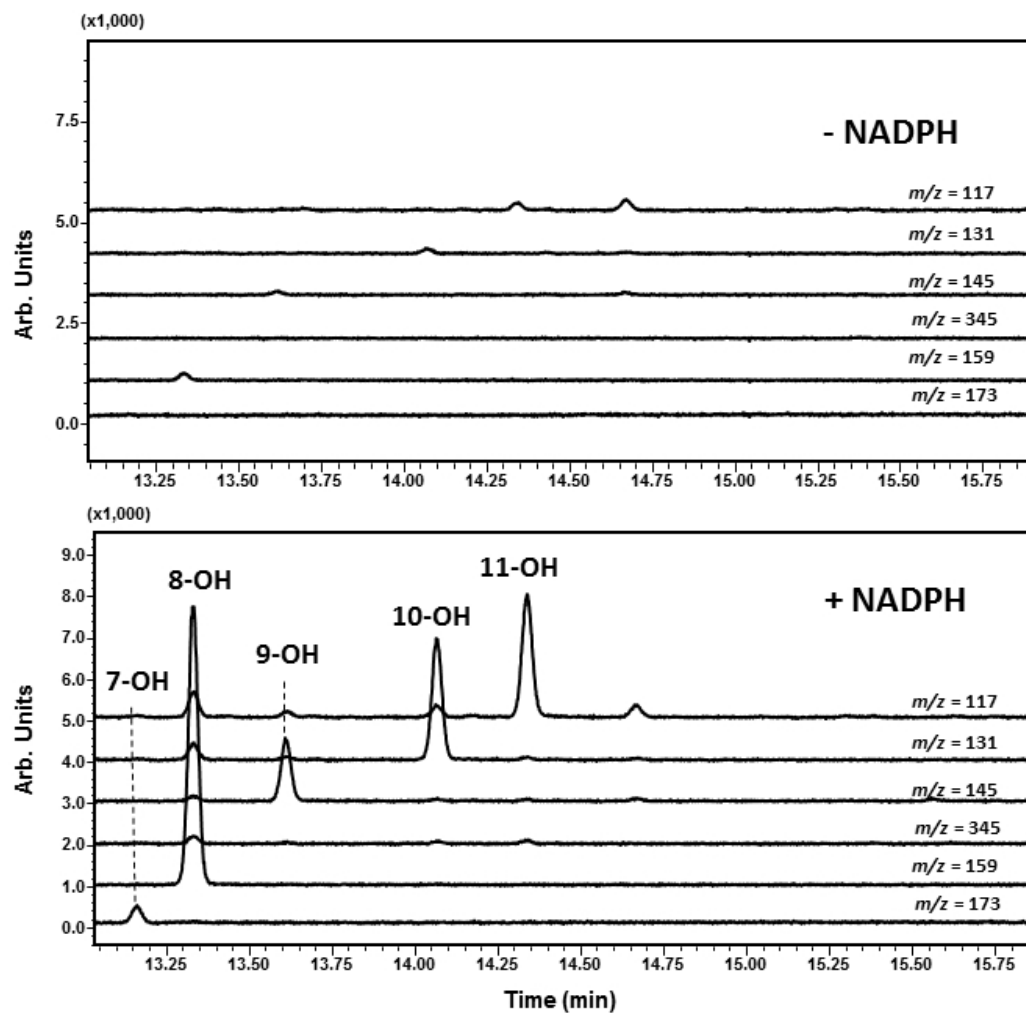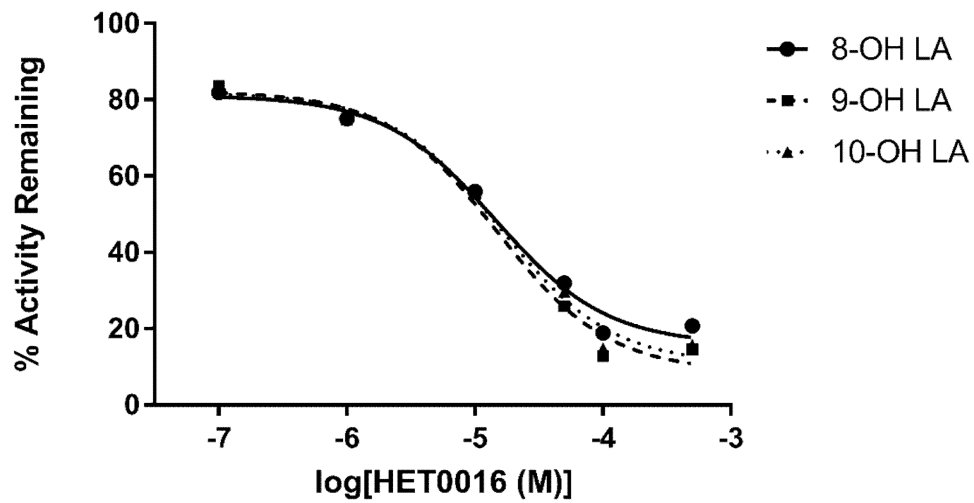
Figure 5.

Figure 6.

A.

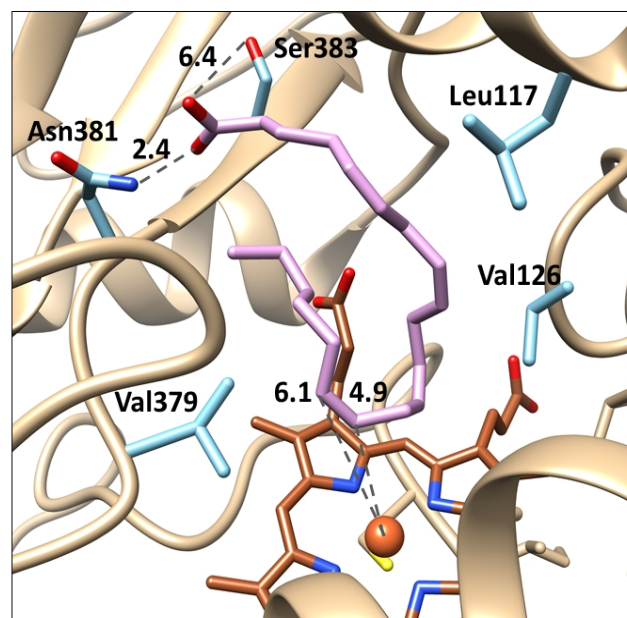**B.**

Supplemental Materials for the following article, submitted for publication in *Drug Metabolism and Disposition*:

Expression and functional characterization of breast cancer-associated cytochrome P450 4Z1 in *Saccharomyces cerevisiae*

Matthew G. McDonald, Sutapa Ray, Clara J. Amorosi, Katherine A. Sitko, John P. Kowalski, Lorela Paco, Abhinav Nath, Byron Gallis, Rheem A. Totah, Maitreya J. Dunham, Douglas M. Fowler and Allan E. Rettie*

Departments of Medicinal Chemistry (MGM, SR JPK, LP, AN, BG, RAT and AER), Genome Sciences (KAS, CJA, MJD and DMF) and Bioengineering (DMF), University of Washington, Seattle, WA 98195.

Supplemental Table 1: Primers used for vector construction

Primers	Sequence 5'-3'
KAS381	gcatctgtgcggtatttcacaccgcataCGACATGGAGGCCCAG
KAS382	gtggtatggtgcactctcagtacaatctgcCAGTATAGCGACCAGCATTCA
KAS378	tatgcggtgtgaaataccgcacagatgcgtaaggagaaaatacc
KAS379	gtggtatggtgcactctcagtacaatctgctctgatgccg

SUPPLEMENTAL FIGURES

Supplemental Figure 1: **Plasmid sequences.**

p416GAL1:

gacgaaagggcctcgtgatacgcctattttttataggttaatgtcatgataataatggtttcttaggacggatcgcttgcctgtaacttacacgcgcctcgtatct

tttaatgatggaataatttgggaatttactctgtgtttatttattttttatgttttgtatttggattttagaaagtaaataaagaaggtagaagagttacggaatgaaga

aaaaaaaataaacaaaggtttaaaaaaatttcaacaaaaagcgtactttacatatatatttattagacaagaaaagcagattaaatagatatacattcgattaac

gataagtaaaatgtaaaatcacaggattttcgtgtgtggtcttctacacagacaagatgaaacaattcggcattaatacctgagagcaggaagagcaagat

aaaaggtagtatttgttggcgatccccctagagtcttttacatcttcggaaaacaaaaactattttttctttaatttctttttttactttctatttttaatttatatatttatat

taaaaaatttaaattataattattttttatagcacgtgatgaaaaggacccaggtggcacttttcggggaaatgtgcgcggaacccctatttgtttatttttctaaat

acattcaaatatgtatccgctcatgagacaataaccctgataaatgcttcaataatattgaaaaaggaagagtatgagtattcaacatttccgtgtcgcccttat

tcccttttttgcggcattttgccttcctgttttttgctcacccagaaacgctggtgaaagtaaaagatgctgaagatcagttgggtgcacgagtgggttacatcg

aactggatctcaacagcggtaagatccttgagagttttcgccccgaagaacgttttccaatgatgagcacttttaaagttctgctatgtggcgcggtattatcc

cgtattgacgccgggcaagagcaactcggtcgccgcatacactattctcagaatgacttggttgagtactcaccagtcacagaaaagcatcttacggatg

gcatgacagtaagagaattatgcagtgctgccataaccatgagtgataacactgcggccaacttacttctgacaacgatcggaggaccgaaggagctaa

ccgcttttttgcacaacatgggggatcatgtaactcgccttgatcgttgggaaccggagctgaatgaagccataccaaacgacgagcgtgacaccacgat

gcctgtagcaatggcaacaacgttgcgcaaactattaactggcgaactacttactctagcttcccggcaacaattaatagactggatggaggcggataaag

ttgcaggaccacttctgcgctcggcccttccggctggctggtttattgctgataaatctggagccggtgagcgtgggtctcgcggtatcattgcagcactgg

ggccagatggtaagccctcccgtatcgtagttatctacacgacggggagtcaggcaactatggatgaacgaaatagacagatcgctgagataggtgcct

cactgattaagcattggtaactgtcagaccaagtttactcatatatactttagattgatttaaaacttcattttttaatttaaaaggatctaggtgaagatcctttttga

taatctcatgaccaaaatcccttaacgtgagttttcgttccactgagcgtcagaccccgtagaaaagatcaaaggatcttcttgagatccttttttttctgcgcgt

aatctgctgcttgcaaacaaaaaaaccaccgctaccagcggtggtttgtttgccggatcaagagctaccaactctttttccgaaggtaactggcttcagcag

agcgcagataccaaatactgtccttctagtgtagccgtagttaggccaccacttcaagaactctgtagcaccgcctacatacctcgctctgctaatcctgtta

ccagtggctgctgccagtggcgataagtcgtgtcttaccgggttggactcaagacgatagttaccggataaggcgcagcggtcgggctgaacggggggg

ttcgtgcacacagcccagcttggagcgaacgacctacaccgaactgagatacctacagcgtgagctatgagaaagcgccacgcttcccgaagggaga

aaggcggacaggtatccggtaagcggcagggtcggaacaggagagcgcacgagggagcttccaggggggaaacgcctggtatctttatagtcctgtcg

ggtttcgccacctctgacttgagcgtcgatttttgtgatgctcgtcagggggggcggagcctatggaaaaacgccagcaacgcggcctttttacggttcctg

gccttttgctggccttttgctcacatgttctttcctgcgttatcccctgattctgtggataaccgtattaccgcctttgagtgagctgataccgctcgccgcagcc

gaacgaccgagcgcagcgagtcagtgagcgaggaagcggaagagcgcccaatacgcaaaccgcctctccccgcgcgttggccgattcattaatgca

gctggcacgacaggtttcccgactggaaagcgggcagtgagcgcaacgcaattaatgtgagttacctcactcattaggcaccccaggctttacactttatg

cttccggctcctatgttgtgtggaattgtgagcggataacaatttcacacaggaaacagctatgaccatgattacgccaagcgcgcaattaaccctcactaa

agggaacaaaagctggagctctagtacggattagaagccgccgagcgggtgacagccctccgaaggaagactctcctccgtgcgtcctcgtcttcacc

ggtcgcgttcctgaaacgcagatgtgcctcgcgccgcactgctccgaacaataaagattctacaatactagctttttatggttatgaagaggaaaaattggca

gtaacctggccccacaaaccttcaaatgaacgaatcaaattaacaaccataggatgataatgcgattagttttttagccttatttctggggtaattaatcagcg

aagcgatgattttttgatctattaacagatatataaatgcaaaaactgcataaccactttaactaatactttcaacattttcggtttgtattacttcttattcaaatgtaa

taaaagtatcaacaaaaaattgttaatatacctctatactttaacgtcaaggagaaaaaaccccggattctagaactagtggatcccccgggctgcaggaat

tcgatatcaagcttatcgataccgtcgacctcgagtcatgtaattagttatgtcacgcttacattcacgccctccccccacatccgctctaaccgaaaaggaa

ggagttagacaacctgaagtctaggtccctatttattttttatagttatgttagtattaagaacgttatttatatttcaaattttctttttttttctgtacagacgcgtgta

cgcatgtaacattatactgaaaaccttgcttgagaaggtttttgggacgctcgaaggctttaatttgcggccggtacccaattcgccctatagtgagtcgtatta

cgcgcgctcactggccgtcgttttacaacgtcgtgactgggaaaaccctggcgttacccaacttaatcgccttgcagcacatccccctttcgccagctggc

gtaatagcgaagaggcccgcaccgatcgcccttcccaacagttgcgcagcctgaatggcgaatggcgcgacgcgccctgtagcggcgcattaagcgc

ggcgggtgtggtggttacgcgcagcgtgaccgctacacttgccagcgccctagcgcccgctcctttcgctttcttcccttcctttctcgccacgttcgccgg

ctttccccgtcaagctctaaatcgggggctccctttagggttccgatttagtgctttacggcacctcgaccccaaaaaacttgattagggtgatggttcacgta

gtgggccatcgccctgatagacggtttttcgccctttgacgttggagtccacgttctttaatagtggactcttgttccaaactggaacaacactcaaccctatct

cggtctattcttttgatttataagggattttgccgatttcggcctattggttaaaaaatgagctgatttaacaaaaatttaacgcgaattttaacaaaatattaacgt

ttacaatttcctgatgcggtattttctccttacgcatctgtgcggtatttcacaccgcatagggtaataactgatataattaaattgaagctctaatttgtgagtttta

gtatacatgcatttacttataatacagttttttagttttgctggccgcatcttctcaaatatgcttcccagcctgctttttctgtaacgttcaccctctaccttagcatcc

cttccctttgcaaatagtcctcttccaacaataataatgtcagatcctgtagagaccacatcatccacggttctatactgttgacccaatgcgtctcccttgtcat

ctaaacccacaccgggtgtcataatcaaccaatcgtaaccttcatctcttccacccatgtctctttgagcaataaagccgataacaaaatctttgtcgctcttcg

caatgtcaacagtacccttagtatattctccagtagatagggagcccttgcatgacaattctgctaacatcaaaaggcctctaggttcctttgttacttcttctgc

cgcctgcttcaaaccgctaacaatacctgggcccaccacaccgtgtgcattcgtaatgtctgcccattctgctattctgtatacacccgcagagtactgcaat

ttgactgtattaccaatgtcagcaaattttctgtcttcgaagagtaaaaaattgtacttggcggataatgcctttagcggcttaactgtgccctccatggaaaaa

4

tcagtcaagatatccacatgtgtttttagtaaacaaattttgggacctaatgcttcaactaactccagtaattccttggtggtacgaacatccaatgaagcacac

aagtttgtttgcttttcgtgcatgatattaaatagcttggcagcaacaggactaggatgagtagcagcacgttccttatatgtagctttcgacatgatttatcttcg

tttcctgcaggttttgttctgtgcagttgggttaagaatactgggcaatttcatgtttcttcaacactacatatgcgtatatataccaatctaagtctgtgctccttc

cttcgttcttccttctgttcggagattaccgaatcaaaaaaatttcaaagaaaccgaaatcaaaaaaaagaataaaaaaaaaaatgatgaattgaattgaaaag

ctgtggtatggtgcactctcagtacaatctgctctgatgccgcatagttaagccagccccgacacccgccaacacccgctgacgcgccctgacgggcttg

tctgctcccggcatccgcttacagacaagctgtgaccgtctccgggagctgcatgtgtcagaggttttcaccgtcatcaccgaaacgcgcga

pUG6:

GAACGCGGCCGCCAGCTGAAGCTTCGTACGCTGCAGGTCGACAACCCTTAATATAACTTCGT

ATAATGTATGCTATACGAAGTTATTAGGTCTAGAGATCTGTTTAGCTTGCCTCGTCCCCGCCG

GGTCACCCGGCCAGCGACATGGAGGCCCAGAATACCCTCCTTGACAGTCTTGACGTGCGCAG

CTCAGGGGCATGATGTGACTGTCGCCCGTACATTTAGCCCATACATCCCCATGTATAATCATT

TGCATCCATACATTTTGATGGCCGCACGGCGCGAAGCAAAAATTACGGCTCCTCGCTGCAGA

CCTGCGAGCAGGGAAACGCTCCCCTCACAGACGCGTTGAATTGTCCCCACGCCGCGCCCCTG

TAGAGAAATATAAAAGGTTAGGATTTGCCACTGAGGTTCTTCTTTCATATACTTCCTTTTAAA

ATCTTGCTAGGATACAGTTCTCACATCACATCCGAACATAAACAACCATGGGTAAGGAAAA

GACTCACGTTTCGAGGCCGCGATTAAATTCCAACATGGATGCTGATTTATATGGGTATAAAT

GGGCTCGCGATAATGTCGGGCAATCAGGTGCGACAATCTATCGATTGTATGGGAAGCCCGAT

GCGCCAGAGTTGTTTCTGAAACATGGCAAAGGTAGCGTTGCCAATGATGTTACAGATGAGAT

GGTCAGACTAAACTGGCTGACGGAATTTATGCCTCTTCCGACCATCAAGCATTTTATCCGTA

CTCCTGATGATGCATGGTTACTCACCACTGCGATCCCCGGCAAAACAGCATTCCAGGTATTA

GAAGAATATCCTGATTCAGGTGAAAATATTGTTGATGCGCTGGCAGTGTTCCTGCGCCGGTT

GCATTCGATTCCTGTTTGTAATTGTCCTTTTAACAGCGATCGCGTATTTCGTCTCGCTCAGGC

GCAATCACGAATGAATAACGGTTTGGTTGATGCGAGTGATTTTGATGACGAGCGTAATGGCT

GGCCTGTTGAACAAGTCTGGAAAGAAATGCATAAGCTTTTGCCATTCTCACCGGATTCAGTC

GTCACTCATGGTGATTTCTCACTTGATAACCTTATTTTTGACGAGGGGAAATTAATAGGTTGT

ATTGATGTTGGACGAGTCGGAATCGCAGACCGATACCAGGATCTTGCCATCCTATGGAACTG

CCTCGGTGAGTTTTCTCCTTCATTACAGAAACGGCTTTTTCAAAAATATGGTATTGATAATCC

TGATATGAATAAATTGCAGTTTCATTTGATGCTCGATGAGTTTTTCTAATCAGTACTGACAAT

AAAAAGATTCTTGTTTTCAAGAACTTGTCATTTGTATAGTTTTTTTATATTGTAGTTGTTCTAT

TTTAATCAAATGTTAGCGTGATTTATATTTTTTTTCGCCTCGACATCATCTGCCCAGATGCGA

AGTTAAGTGCGCAGAAAGTAATATCATGCGTCAATCGTATGTGAATGCTGGTCGCTATACTG

CTGTCGATTCGATACTAACGCCGCCATCCAGTGTCGAAAACGAGCTCTCGAGAACCCTTAAT

ATAACTTCGTATAATGTATGCTATACGAAGTTATTAGGTGATATCAGATCCACTAGTGGCCT

ATGCGGCCGCGGATCTGCCGGTCTCCCTATAGTGAGTCGTATTAATTTCGATAAGCCAGGTT

AACCTGCATTAATGAATCGGCCAACGCGCGGGGAGAGGCGGTTTGCGTATTGGGCGCTCTTC

CGCTTCCTCGCTCACTGACTCGCTGCGCTCGGTCGTTCGGCTGCGGCGAGCGGTATCAGCTC

ACTCAAAGGCGGTAATACGGTTATCCACAGAATCAGGGGATAACGCAGGAAAGAACATGTG

AGCAAAAGGCCAGCAAAAGGCCAGGAACCGTAAAAAGGCCGCGTTGCTGGCGTTTTTCCAT

AGGCTCCGCCCCCCTGACGAGCATCACAAAAATCGACGCTCAAGTCAGAGGTGGCGAAACC

CGACAGGACTATAAAGATACCAGGCGTTTCCCCCTGGAAGCTCCCTCGTGCGCTCTCCTGTT

CCGACCCTGCCGCTTACCGGATACCTGTCCGCCTTTCTCCCTTCGGGAAGCGTGGCGCTTTCT

CAATGCTCACGCTGTAGGTATCTCAGTTCGGTGTAGGTCGTTCGCTCCAAGCTGGGCTGTGT

GCACGAACCCCCCGTTCAGCCCGACCGCTGCGCCTTATCCGGTAACTATCGTCTTGAGTCCA

ACCCGGTAAGACACGACTTATCGCCACTGGCAGCAGCCACTGGTAACAGGATTAGCAGAGC

GAGGTATGTAGGCGGTGCTACAGAGTTCTTGAAGTGGTGGCCTAACTACGGCTACACTAGAA

GGACAGTATTTGGTATCTGCGCTCTGCTGAAGCCAGTTACCTTCGGAAAAAGAGTTGGTAGC

TCTTGATCCGGCAAACAAACCACCGCTGGTAGCGGTGGTTTTTTTGTTTGCAAGCAGCAGAT

TACGCGCAGAAAAAAAGGATCTCAAGAAGATCCTTTGATCTTTTCTACGGGGTCTGACGCTC

AGTGGAACGAAAACTCACGTTAAGGGATTTTGGTCATGAGATTATCAAAAAGGATCTTCACC

TAGATCCTTTTAAATTAAAAATGAAGTTTTAAATCAATCTAAAGTATATATGAGTAAACTTG

GTCTGACAGTTACCAATGCTTAATCAGTGAGGCACCTATCTCAGCGATCTGTCTATTTCGTTC

6

ATCCATAGTTGCCTGACTCCCCGTCGTGTAGATAACTACGATACGGGAGGGCTTACCATCTG

GCCCCAGTGCTGCAATGATACCGCGAGACCCACGCTCACCGGCTCCAGATTTATCAGCAATA

AACCAGCCAGCCGGAAGGGCCGAGCGCAGAAGTGGTCCTGCAACTTTATCCGCCTCCATCC

AGTCTATTAATTGTTGCCGGGAAGCTAGAGTAAGTAGTTCGCCAGTTAATAGTTTGCGCAAC

GTTGTTGCCATTGCTACAGGCATCGTGGTGTCACGCTCGTCGTTTGGTATGGCTTCATTCAGC

TCCGGTTCCCAACGATCAAGGCGAGTTACATGATCCCCCATGTTGTGCAAAAAAGCGGTTAG

CTCCTTCGGTCCTCCGATCGTTGTCAGAAGTAAGTTGGCCGCAGTGTTATCACTCATGGTTAT

GGCAGCACTGCATAATTCTCTTACTGTCATGCCATCCGTAAGATGCTTTTCTGTGACTGGTGA

GTACTCAACCAAGTCATTCTGAGAATAGTGTATGCGGCGACCGAGTTGCTCTTGCCCGGCGT

CAATACGGGATAATACCGCGCCACATAGCAGAACTTTAAAAGTGCTCATCATTGGAAAACG

TTCTTCGGGGCGAAAACTCTCAAGGATCTTACCGCTGTTGAGATCCAGTTCGATGTAACCCA

CTCGTGCACCCAACTGATCTTCAGCATCTTTTACTTTCACCAGCGTTTCTGGGTGAGCAAAAA

CAGGAAGGCAAAATGCCGCAAAAAAGGGAATAAGGGCGACACGGAAATGTTGAATACTCA

TACTCTTCCTTTTTCAATATTATTGAAGCATTTATCAGGGTTATTGTCTCATGAGCGGATACA

TATTTGAATGTATTTAGAAAAATAAACAAATAGGGGTTCCGCGCACATTTCCCCGAAAAGTG

CCACCTGACGTCTAAGAAACCATTATTATCATGACATTAACCTATAAAAATAGGCGTATCAC

GAGGCCCTTTCGTCTCGCGCGTTTCGGTGATGACGGTGAAAACCTCTGACACATGCAGCTCC

CGGAGACGGTCACAGCTTGTCTGTAAGCGGATGCCGGGAGCAGACAAGCCCGTCAGGGCGC

GTCAGCGGGTGTTGGCGGGTGTCGGGGCTGGCTTAACTATGCGGCATCAGAGCAGATTGTAC

TGAGAGTGCACCATATGGACATATTGTCGTTAGAACGCGGCTACAATTAATACATAACCTTA

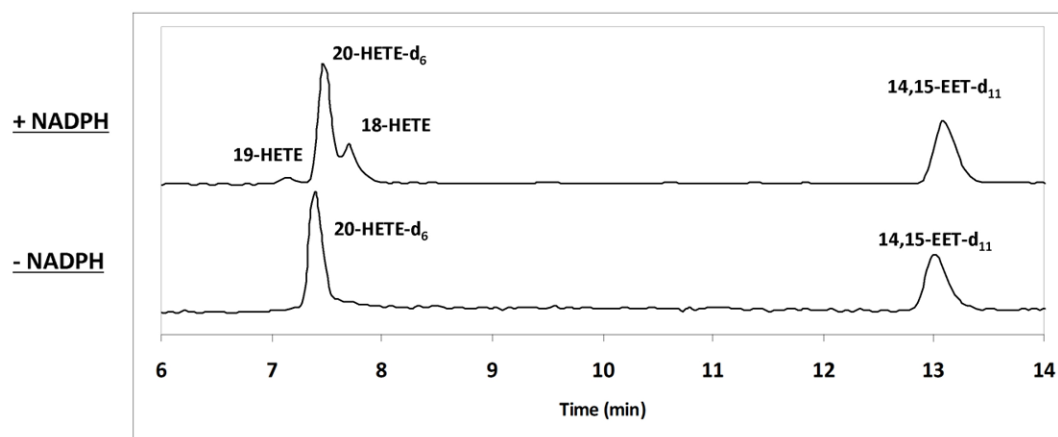TGTATCATACACATACGATTTAGGTGACACTATA

p41KGAL1

gacgaaagggcctcgtgatacgcctattttttataggttaatgtcatgataataatggtttcttaggacggatcgcttgcctgtaacttacacgcgcctcgtatct

tttaatgatggaataatttgggaatttactctgtgtttatttattttttatgttttgtatttggattttagaaagtaaataaagaaggtagaagagttacggaatgaaga

aaaaaaaataaacaaaggtttaaaaaatttcaacaaaaagcgtactttacatatatatttattagacaagaaaagcagattaaatagatatacattcgattaac

gataagtaaaatgtaaaatcacaggattttcgtgtgtggtcttctacacagacaagatgaaacaattcggcattaatacctgagagcaggaagagcaagat

7

aaaaggtagtatttgttggcgatcccccctagagtcttttacatcttcggaaaacaaaaactattttttctttaatttctttttttactttctattttttaatttatatatttatat

taaaaaatttaaattataattattttttatagcacgtgatgaaaaggacccaggtggcacttttcggggaaatgtgcgcggaaccccctatttgtttattttttctaaat

acattcaaatatgtatccgctcatgagacaataaccctgataaatgcttcaataatattgaaaaaggaagagtatgagtattcaacatttccgtgtcgcccttat

tcccttttttgcggcattttgccttcctgttttttgctcacccagaaacgctggtgaaagtaaaagatgctgaagatcagttgggtgcacgagtgggttacatcg

aactggatctcaacagcggtaagatccttgagagttttcgccccgaagaacgttttccaatgatgagcacttttaaagttctgctatgtggcgcggtattatcc

cgtattgacgccgggcaagagcaactcggtcgccgcatacactattctcagaatgacttggttgagtactcaccagtcacagaaaagcatcttacggatg

gcatgacagtaagagaattatgcagtgctgccataaccatgagtgataacactgcggccaacttacttctgacaacgatcggaggaccgaaggagctaa

ccgcttttttgcacaacatggggggatcatgtaactcgccttgatcgttgggaaccggagctgaatgaagccataccaaacgacgagcgtgacaccacgat

gcctgtagcaatggcaacaacgttgcgcaaactattaactggcgaactacttactctagcttcccggcaacaattaatagactggatggaggcggataaag

ttgcaggaccacttctgcgctcggcccttccggctggctggtttattgctgataaatctggagccggtgagcgtgggtctcgcggtatcattgcagcactgg

ggccagatggtaagccctcccgtatcgtagttatctacacgacggggagtcaggcaactatggatgaacgaaatagacagatcgctgagataggtgcct

cactgattaagcattggtaactgtcagaccaagtttactcatatatactttagattgatttaaaacttcattttaatttaaaaggatctaggtgaagatcctttttga

taatctcatgaccaaaatcccttaacgtgagttttcgttccactgagcgtcagacccgtagaaaagatcaaaggatcttcttgagatcctttttttctgcgcgt

aatctgctgcttgcaaacaaaaaaccaccgctaccagcggtggtttgtttgccggatcaagagctaccaactctttttccgaaggtaactggcttcagcag

agcgcagataccaaatactgtccttctagtgtagccgtagttaggccaccacttcaagaactctgtagcaccgcctacatacctcgctctgctaatcctgtta

ccagtggctgctgccagtggcgataagtcgtgtcttaccgggttggactcaagacgatagttaccggataaggcgcagcggtcgggctgaacggggggg

ttcgtgcacacagcccagcttggagcgaacgacctacaccgaactgagatacctacagcgtgagctatgagaaagcgccacgcttcccgaagggaga

aaggcggacaggtatccggtaagcggcagggtcggaacaggagagcgcacgagggagcttccagggggaaacgcctggtatctttatagtcctgtcg

ggtttcgccacctctgacttgagcgtcgatttttgtgatgctcgtcaggggggcggagcctatggaaaaacgccagcaacgcggcctttttacggttcctg

gccttttgctggccttttgctcacatgttctttcctgcgttatcccctgattctgtggataaccgtattaccgcctttgagtgagctgataccgctcgccgcagcc

gaacgaccgagcgcagcgagtcagtgagcgaggaagcggaagagcgcccaatacgcaaaccgcctctccccgcgcgttggccgattcattaatgca

gctggcacgacaggtttcccgactggaaagcgggcagtgagcgcaacgcaattaatgtgagttacctcactcattaggcaccccaggctttacactttatg

cttccggctcctatgttgtgtggaattgtgagcggataacaatttcacacaggaaacagctatgaccatgattacgccaagcgcgcaattaaccctcactaa

agggaacaaaagctggagctctagtacggattagaagccgccgagcgggtgacagccctccgaaggaagactctcctccgtgcgtcctcgtcttcacc

ggtcgcgttcctgaaacgcagatgtgcctcgcgccgcactgctccgaacaataaagattctacaatactagcttttatggttatgaagaggaaaaattggca

gtaacctggccccacaaaccttcaaatgaacgaatcaaattaacaaccataggatgataatgcgattagttttttagccttatttctggggtaattaatcagcg
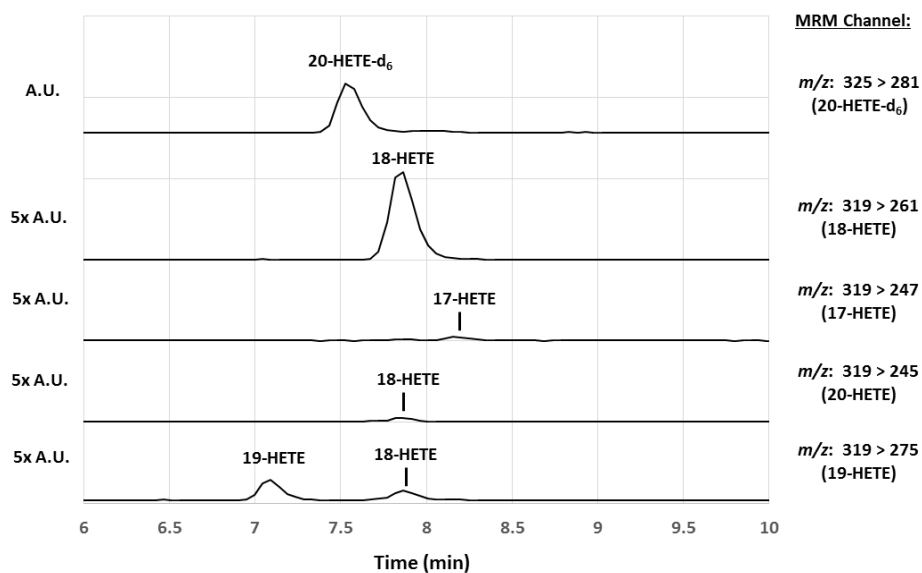
aagcgatgattttgatctattaacagatatataaatgcaaaaactgcataaccactttaactaatactttcaacattttcggtttgtattacttcttattcaaatgtaa

taaaagtatcaacaaaaaattgttaatatacctctatactttaacgtcaaggagaaaaaaccccggattctagaactagtggatcccccgggctgcaggaat

tcgatatcaagcttatcgataccgtcgacctcgagtcatgtaattagttatgtcacgcttacattcacgccctcccccacatccgctctaaccgaaaaggaa

ggagttagacaacctgaagtctaggtccctatttatttttttatagttatgttagtattaagaacgttatttatatttcaaattttctttttttttctgtacagacgcgtgta

cgcatgtaacattatactgaaaaccttgcttgagaaggtttttgggacgctcgaaggctttaatttgcggccggtacccaattcgccctatagtgagtcgtatta

cgcgcgctcactggccgtcgttttacaacgtcgtgactgggaaaaccctggcgttacccaacttaatcgccttgcagcacatccccctttcgccagctggc

gtaatagcgaagaggcccgcaccgatcgcccttcccaacagttgcgcagcctgaatggcgaatggcgcgacgcgccctgtagcggcgcattaagcgc

ggcgggtgtggtggttacgcgcagcgtgaccgctacacttgccagcgccctagcgcccgctcctttcgctttcttcccttcctttctcgccacgttcgccgg

ctttccccgtcaagctctaaatcgggggctccctttagggttccgatttagtgctttacggcacctcgaccccaaaaaacttgattagggtgatggttcacgta

gtgggccatcgccctgatagacggtttttcgccctttgacgttggagtccacgttctttaatagtggactcttgttccaaactggaacaacactcaaccctatct

cggtctattcttttgatttataagggattttgccgatttcggcctattggttaaaaaatgagctgatttaacaaaaatttaacgcgaattttaacaaaatattaacgt

ttacaatttcctgatgcggtattttctccttacgcatctgtgcggtatttcacaccgcata CGACATGGAGGCCCAGAATACCCTCCT

TGACAGTCTTGACGTGCGCAGCTCAGGGGCATGATGTGACTGTCGCCCGTACATTTAGCCCA

TACATCCCCATGTATAATCATTTGCATCCATACATTTTGATGGCCGCACGGCGCGAAGCAAA

AATTACGGCTCCTCGCTGCAGACCTGCGAGCAGGGAAACGCTCCCCTCACAGACGCGTTGAA

TTGTCCCCACGCCGCGCCCCTGTAGAGAAATATAAAAGGTTAGGATTTGCCACTGAGGTTCT

TCTTTCATATACTTCCTTTTAAAATCTTGCTAGGATACAGTTCTCACATCACATCCGAACATA

AACAACCATGGGTAAGGAAAAGACTCACGTTTCGAGGCCGCGATTAAATTCCAACATGGAT

GCTGATTTATATGGGTATAAATGGGCTCGCGATAATGTCGGGCAATCAGGTGCGACAATCTA

TCGATTGTATGGGAAGCCCGATGCGCCAGAGTTGTTTCTGAAACATGGCAAAGGTAGCGTTG

CCAATGATGTTACAGATGAGATGGTCAGACTAAACTGGCTGACGGAATTTATGCCTCTTCCG

ACCATCAAGCATTTTATCCGTACTCCTGATGATGCATGGTTACTCACCACTGCGATCCCCGGC

AAAACAGCATTCCAGGTATTAGAAGAATATCCTGATTCAGGTGAAAATATTGTTGATGCGCT

GGCAGTGTTCCTGCGCCGGTTGCATTCGATTCCTGTTTGTAATTGTCCTTTTAACAGCGATCG

CGTATTTCGTCTCGCTCAGGCGCAATCACGAATGAATAACGGTTTGGTTGATGCGAGTGATT

TTGATGACGAGCGTAATGGCTGGCCTGTTGAACAAGTCTGGAAAGAAATGCATAAGCTTTTG

9

CCATTCTCACCGGATTCAGTCGTCACTCATGGTGATTTCTCACTTGATAACCTTATTTTTGAC

GAGGGGAAATTAATAGGTTGTATTGATGTTGGACGAGTCGGAATCGCAGACCGATACCAGG

ATCTTGCCATCCTATGGAACTGCCTCGGTGAGTTTTCTCCTTCATTACAGAAACGGCTTTTC

AAAAATATGGTATTGATAATCCTGATATGAATAAATTGCAGTTTCATTTGATGCTCGATGAG

TTTTTCTAATCAGTACTGACAATAAAAAGATTCTTGTTTTCAAGAACTTGTCATTTGTATAGT

TTTTTATATTGTAGTTGTTCTATTTTAATCAAATGTTAGCGTGATTTATATTTTTTTCGCCTC

GACATCATCTGCCCAGATGCGAAGTTAAGTGCGCAGAAAGTAATATCATGCGTCAATCGTAT

GTGAATGCTGGTCGCTATACTGgtggtatggtgcactctcagtacaatctgctctgatgccgcatagttaagccagcccccgacaccc

gccaacacccgctgacgcgccctgacgggcttgtctgctcccggcatccgcttacagacaagctgtgaccgtctccgggagctgcatgtgtcagaggttt

tcaccgtcatcaccgaaacgcgcga

A.

B.

Supplemental Figure 2: **ESI^{-} LC-MS/MS chromatograms showing AA metabolism by CYP4F12**

Supersomes. A). Total ion chromatograms (TICs) of metabolites produced from incubations of 75 µM

11

AA with CYP4F12 Supersomes in the presence and absence of NADPH. TICs = sum of 19 individual AA metabolite MRM channels plus channels for the internal standards, 20-HETE-d_6 and 14,15-EET-d_{11} (i.e. the same 19 channels used in the analysis of CYP4Z1-mediated AA metabolism plus additional channels for the analysis of 17-HETE and 18-HETE). Turnover rates for CYP4F12 AA metabolites: 18-HETE = 0.099 ± 0.001 pmol/min/pmol; 19-HETE = 0.031 ± 0.002 pmol/min/pmol; B). Magnifications of individual MRM chromatograms from a (+) NADPH incubation of CYP4F12 Supersomes with AA (the amplitudes for the individual metabolite MRM chromatogram peaks are normalized to 5x the scale of the internal standard 20-HETE-d_6 peak, in arbitrary units). MRM channels: 20-HETE-d_6 ($m/z = 325 > 281$); 17-HETE ($m/z = 319 > 247$), 18-HETE ($m/z = 319 > 261$), 20-HETE ($m/z = 319 > 245$), 19-HETE ($m/z = 319 > 275$). The minor peak at 8.2 min in (B) is presumed to be 17-HETE based on its LC-MS/MS profile (i.e. the M-72 daughter ion should be specific to the ω-4 AA monohydroxy metabolite due to the neutral loss of a $CH_3CH_2CH_2CHO$ fragment), however we are unable to confirm the metabolite's identity (or quantify it), because we lack a 17-HETE synthetic standard.

Note: While the major daughter ion for 18-HETE occurs at M-58 (m/z 261), this metabolite also produces minor fragment ions at m/z 245 and m/z 275 that can be seen in the 19-HETE and 20-HETE channels. The peak area ratios for the MRM channels m/z 319 > 275 : 319 > 245, determined from an 18-HETE standard calibration curve, is ~2.5 and matches the ratio observed here for the 18-HETE metabolite peaks. By contrast, 20-HETE consistently produces a ratio of ~1.0 for these same MRM peaks under standard experimental conditions. From this observation, we can determine that the peak at m/z 319 > 245 (20-HETE channel) is mostly, if not entirely, due to 18-HETE, rather than 20-HETE which might overlap with the 18-HETE signal. Taken together with the low relative amplitude of the peak in the m/z 319 > 245 channel in comparison to other signals, we conclude from this data that little to no 20-HETE is produced in this reaction.
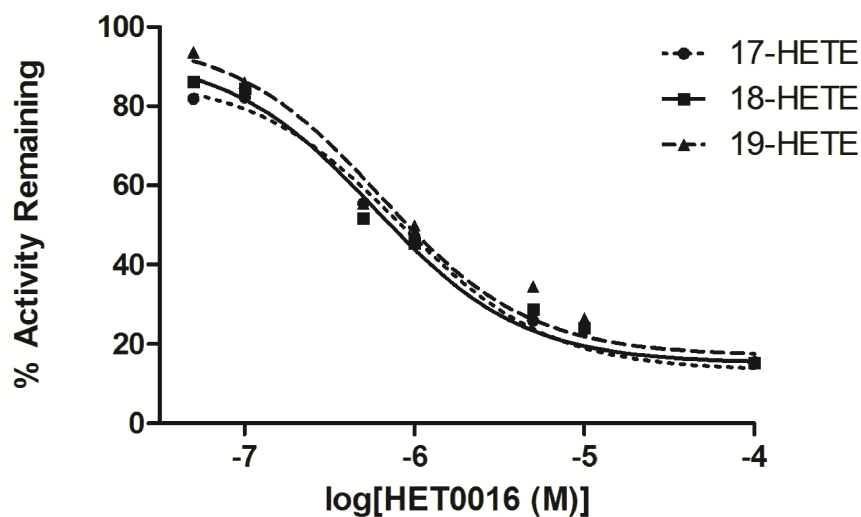
Supplemental Figure 3: HET0016 inhibition of CYP4F12-catalyzed AA metabolism. The overlaid graphs show the relative IC_{50} curves for inhibition of CYP4F12-mediated AA 17-, 18- and 19-hydroxylase activity by HET0016. Data points denote the mean turnover rate of AA to each metabolite, obtained from duplicate incubations of 75 μM AA and HET0016 (at concentrations ranging from 0.1 – 500 μM) with CYP4F12 Supersomes, expressed as a percentage of the rate obtained in the absence of inhibitor. HET0016 inhibited formation of 17-HETE, 18-HETE and 19-HETE with IC_{50} values of 0.82, 0.58 and 0.63 μM, respectively.